A Novel Hybrid Vehicle Architecture: Modeling, Simulation and Experiments

A Thesis

Submitted for the Degree of

Doctor of Philosophy

in the **Faculty of Engineering**

by

Raviteja Chanumolu

Mechanical Engineering
Indian Institute of Science
Bangalore – 560 012 (INDIA)

July 2016

DEDICATED TO

my wife Tejaswini, parents, friends and advisor

who have been with me all along and at all times

CERTIFICATE

I hereby certify that the content embodied in this thesis titled **A Novel Hybrid Vehicle Architecture: Modeling, Simulation and Experiments** has been carried out by Mr. Raviteja Chanumolu at the Indian Institute of Science, Bangalore under my supervision and that it has not been submitted elsewhere for the award of any degree or diploma.

Signature of the Thesis Supervisor: .....

Professor Ashitava Ghosal
Dept. of Mechanical Engineering
Indian Institute of Science, Bangalore

DECLARATION

I hereby declare that the content embodied in this thesis titled **A Novel Hybrid Vehicle Architecture: Modeling, Simulation and Experiments** is the research carried out by me at the Department of Mechanical Engineering, Indian Institute of Science, Bangalore under the supervision Prof. Ashitava Ghosal, Department of Mechanical Engineering, IISc. In keeping with the general practice in reporting scientific observations, due acknowledgement has been made wherever the work described is based on the findings of other investigations.

Signature of the Author: .....

Raviteja Chanumolu
Dept. of Mechanical Engineering
Indian Institute of Science, Bangalore

Acknowledgements

I am deeply grateful to my advisor, Prof. Ashitava Ghosal, for the guidance and support during the past five years. I feel incredibly fortunate for the opportunity to work with him. I would also like to express my deepest gratitude to the Department of Mechanical Engineering, Indian Institute of Science for all the help during this research work.

This research is partly funded by a grant from GM R&D, Warren, Michigan.I wish to thank Dr. Madhu Raghavan and Mr. V. Prasad Atluri, Power train research lab, Warren, Michigan, USA for their extensive and timely help in providing engine data and in modeling. I would also like to thank Prof. Ravikrishna and Dr. Himabindu for providing the lab facility for experimental setup and Prof. N.V.C. Rao of CEDT department for his valuable inputs at the initial stages of my project. I am also grateful to the many bright students and researchers I met at IISc for the interesting discussions. I would like to thank my lab mates Sandeep, Ashith, Midhun, Bharat, Puneet, Ashwin, Mohith, Arkadeep and Sudhir for their support.

Finally, I would like to thank my family for being always so close to me despite the geographical distance. I could not have made it without them supporting me all along.

Abstract

Electric and hybrid vehicles are particularly suited for use in urban areas since city transportation is mainly characterized by relatively short driving distances, low continuous power requirements, long idling times and high availability of regenerative braking energy. These characteristics, when carefully incorporated into the design process, create valuable opportunities for developing clean, efficient and cost effective urban vehicle propulsion systems.

In the first part of the thesis, we present data collected in the city of Bangalore, India from a very commonly seen mode of transportation for hire in India and other emerging economies, namely a three-wheeled vehicle known as the "auto-rickshaw". From a statistical analysis, it is shown that the typical range is 72.5 km with a mean speed of 12.5 km/h. More than 60% of the time the auto-rickshaw is stationary or has a speed of less that 5 km/h. From a model of the auto-rickshaw, it is shown from simulations that 4 kW DC motor and about 10 kWh of electrical energy is enough to meet 80% of typical requirement. Based on this finding, in this thesis, a novel parallel hybrid architecture is proposed where two 2 kW DC hub motors are directly mounted on the wheels and an internal combustion (IC) engine output is connected to the stator of the DC hub motors to provide additional power when required. To match load and speed, a continuously variable transmission (CVT) is placed in-between the IC engine and the DC hub motor. The proposed hybrid configuration adds speed to the wheel output unlike the normal power split configuration which adds torque.

One of the the main objective of this work is to study and compare the performance of the above novel speed-addition and compare with the typical torque-addition configuration. A MATLAB/Simulink model for both the configurations, with DC hub motor and a small IC engine, has been created and the fuel consumption has been calculated. It is shown that the proposed speed-addition concept gives better fuel efficiency for the standard modified Indian Driving Cycle. The models have also been compared for actual driving data and an optimal control strategy has been developed using dynamic programming. It is again shown that the proposed speed-addition concept results in better fuel economy.

In the last part of the thesis, a low cost experimental test-bed consisting of an auto-rickshaw

Abstract

IC engine, a CVT and a 2 kW DC hub motor has been developed to validate the speed-addition concept and compare with the torque-addition configuration. The torque-speed curves of the IC engine, the DC motor and both of them together, in the speed and torque-addition configuration, have been obtained. It is shown that the speed-addition concept does indeed work and the obtained results are significantly different from the torque-addition configuration.

Contents

List of Figures

List of Tables

LIST OF TABLES

Chapter 1

Introduction

The fossil fuel based automobile industry currently faces three main concerns in the form of air pollution, global warming due to carbon emission and depleting petroleum reserves. The costs associated with these concerns are huge and involve financial, human or both aspects [1]. The newer petroleum reserves that are being found are expensive to exploit and limited in number whereas the consumption of fuel is increasing at an alarming rate, especially in emerging economies, and according to the estimates the oil reserves of the world may be depleted in the near future [2]. Fossil fuel-burning transportation vehicles are some of the largest remaining contributors to air pollution [3]. In the crowded urban environments of the emerging economies, vehicles generally move at a very low speed, have limited range, halt frequently due to congestion or traffic and resulting in idling of IC engines which in turn leads to low fuel economy and urban pollution. These aspects make electric vehicles an ideal choice for urban transportation. However, efficient and low cost storage of the required energy in batteries and by other means is still an issue and hybrid electric vehicles are expected to be an good option in the near term.

In this Chapter, we present a brief history of hybrid vehicles, give a brief overview of existing state-of- the-art in hybrid electric vehicle architectures and various energy management processes with emphasis on hybrid three-wheeled vehicles and also address the need and motivation for the development of low cost hybrid propulsion architecture.

1.1 Hybrid vehicles – history and classification

Hybrid electric vehicles in some form or other has been around for more than 100 years. Some of the important dates and events in the development of hybrid vehicles according to Hybrid cars website are as follows:

- In 1898 Dr. Ferdinand Porsche built his first car, the Lohner Electric Chaise [4]. The first prototypes were two-wheel drive, battery-powered electric vehicles with two front wheel hub-mounted motors. A later version, now termed as a series hybrid, used hub-mounted electric motors in each wheel and an internal combustion engine to spin a generator that provided power to electric motors located in the wheel hubs. On battery alone, the car could travel nearly 40 miles(64.4 km).

- By 1900, American car companies had made 1681 steam, 1575 electric, and 936 gasoline cars. In the first few years of the 20th century, thousands of electric and hybrid cars were produced. The car, made in 1903 by the Krieger company, used a gasoline engine to supplement a battery pack [5].

- In 1900, a Belgian car maker, Pieper, introduced a 3.5 horsepower(2.6 kW) voiturette in which the small gasoline engine was mated to an electric motor under the seat. When the car was cruising, its electric motor was in effect a generator, recharging the batteries. When the car was climbing a grade, the electric motor, mounted coaxially with the gas engine, gave it a boost. The Pieper patents were used by a Belgium firm, Auto-Mixte, to build commercial vehicles from 1906 to 1912 [6].

- The Electric Vehicle Company built 2000 taxicabs, trucks, and buses, and set up subsidiary cab and car rental companies from New York to Chicago. Smaller companies, representing approximately 57 auto plants, turned out about 4000 cars [7].

- In 1904, Henry Ford overcame the challenges posed by gasoline-powered cars- noise, vibration, and odor - and began assembly-line production of low-priced, lightweight, gas-powered vehicles. Henry Fords assembly line and the advent of the self-starting gas engine signaled a rapid decline in hybrid cars by 1920. Within a few years, the electric vehicle company failed [6].

- In 1905, an American engineer named H. Piper filed a patent for a petrol-electric hybrid vehicle. His idea was to use an electric motor to assist an IC engine, enabling it to achieve 25 mph(40 km/h) [4].

- In 1916, two prominent electric vehicle makers, Baker of Cleveland and Woods of Chicago, offered hybrid cars. Woods claimed that their hybrid reached a top speed of 35 mph(56 km/h) and achieved fuel efficiency of 48 mpg(20.41 km/l). The Woods Dual Power was more expensive and less powerful than its gasoline competition and therefore sold poorly [6].

- In 1970s, with the Arab oil embargo of 1973, the price of gasoline soared, creating new interest in electric vehicles. The U.S. Department of Energy ran tests on many electric and hybrid vehicles produced by various manufacturers, including a hybrid known as the VW Taxi produced by Volkswagen in Wolfsburg, West Germany [8]. The taxi, which used a parallel hybrid configuration allowing flexible switching between the gasoline engine and electric motor, logged over 13,000 kilometers on the road, and was shown at auto shows throughout Europe and the United States.

- Briggs and Stratton, the company known for manufacturing lawn mower engines, developed a hybrid car powered by a twin cylinder four-stroke 12 kW gasoline engine and an electric motorfor total of 19 kW. The hybrid drivetrain provided power for a custom-designed two-door vehicle with six wheelstwo in front and four in the back [4].

- Audi unveiled the first generation of the Audi Duo experimental vehicle, based on the Audi 100 Avant Quattro. The car had a 12.6 horsepower electric engine, which drove the rear wheels instead of a propeller shaft. A nickel-cadmium battery supplied the energy. The front-wheel drive was powered by a 2.3-litre five-cylinder engine with an output of 136 horsepower. Two years later, Audi unveiled the second generation Duo, also based on the Audi 100 Avant quattro.

- The world started down a new road in 1997 when the first modern hybrid electric car, the Toyota Prius, was sold in Japan. Two years later, the U.S. saw its first sale of a hybrid, the Honda Insight. These two vehicles, followed by the Honda Civic hybrid, marked a radical change in the type of car being offered to the public: vehicles that bring some of the benefits of battery electric vehicles into the conventional gasoline powered cars and trucks we have been using for more than 100 years. Along the line, over 20 models of passenger hybrids have been introduced to the auto market [4].

Hybrid vehicles can be classified based on the degree of hybridization. In case of hybrid electric vehicle the amount of load that can be distributed between electric motor and IC engine defines the hybridization. These can be broadly classified as:

Full hybrid

In this type of hybrid the engine as well as the electric motor both are powerful enough to power the vehicle independently. The main challenge lies in the optimum utilization of both the power sources based on drive cycle. Other smart power saving features like start-stop system, regenerative braking etc. are also included. The common example for full hybrid is

Toyota Camry, Toyota Prius and Chevy volt. Many other automakers are also introducing full hybrid vehicles.

Mild hybrid

In this type of hybrid a small DC motor (stator/generator) is coupled in parallel with the main IC engine. The additional DC motor provides assistance to the IC engine as and when required. The DC motor makes use of the battery which is replenished by regenerative braking. It also uses start-stop system, but The DC motor alone cannot be used to power the vehicle. There are many mild hybrids being introduced into Indian market such as Maruthi Suzuki Ciaz, Ertiga and the classic example for mild hybrid in international market is Honda Insight with integrated motor assist and Chevrolet brands with e-assist.

Micro hybrids

Micro hybrids are not a hybrid in true sense as the vehicle only runs on IC engine. However, these feature a start-stop system and regenerative braking. In this type of vehicles the IC engine is switched off during engine idling with the accessories running on battery power. The IC engine starts again when the vehicle starts moving or battery level falls below the defined threshold level. Many vehicles in Indian market such as Mercedes Benz ML250, Mahindra Scorpio include mild hybrid features.

The hybrid electric vehicle can also be classified based on the drivetrain structure. These are:

Parallel hybrid

In a parallel hybrid, the power can flow in parallel to the wheels from either the batteries or the IC engine or from both. An electronic controller can sense the load and speed of the wheel/vehicle and using built-in algorithms, the power can be made to flow to the wheels appropriately. In most urban driving (especially in crowded and narrow streets in less developed countries), the peak power is rarely required. In such situations, the parallel hybrid can be configured in a way such that most of the time, the vehicle runs on batteries resulting in low emissions and high fuel efficiency. Only when required, power can be added to the wheels from the IC engine. In this framework, the IC engine, the batteries and generator, and the electric motor need not be individually designed to meet peak requirements. This makes a parallel hybrid configuration potentially much cheaper and promising. A schematic of a parallel hybrid configuration is shown in figure 1.1.

An addition advantage of a parallel hybrid vehicle is that the system has the ability to offer

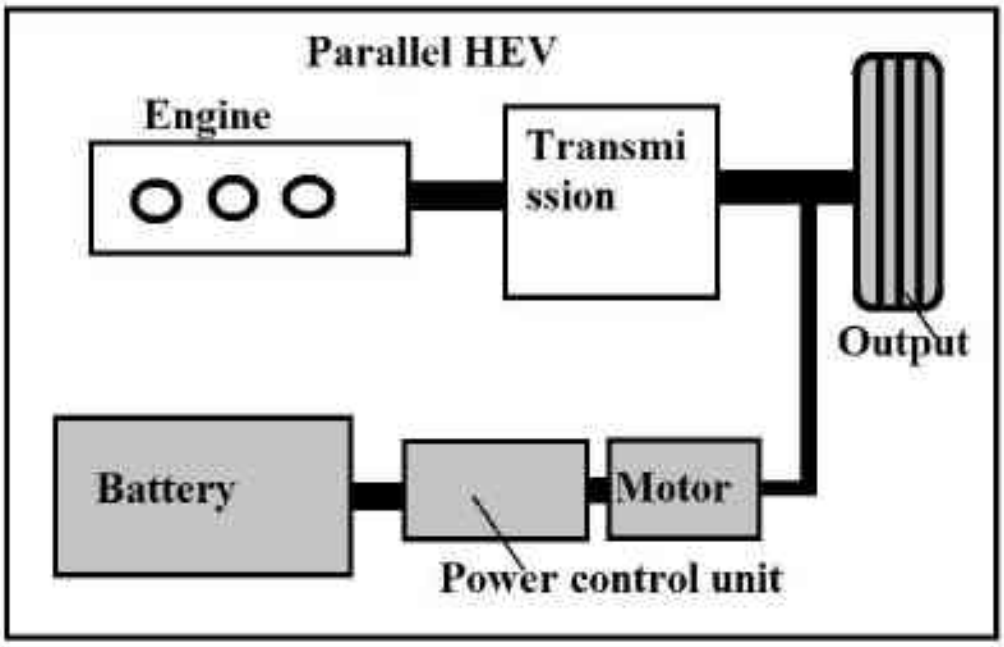

Figure 1.1: Schematic of a parallel hybrid electric vehicle

higher efficiency during highway driving condition. During highway driving, the vehicle speed does not vary significantly and therefore it is more efficient to drive the wheels directly from the IC engine. In addition, the electric motor can be used solely during city driving while the IC engine recharges the battery, thus providing higher overall efficiency. In addition, both power sources can be utilized simultaneously to provide maximum performance of the vehicle. The main disadvantage is in the added complication of designing power trains where power can be added and the use of a sophisticated electronic controller.

Series hybrid

In a series hybrid the IC engine runs an electric generator which produces electricity to charge batteries. The batteries drive the electric motor to propel the vehicle – the arrangement is similar in principle to the well known diesel-electric locomotives. Since the engine does not 'see' the wheel, it can be made to run at an optimized operating condition (best in terms of fuel efficiency and emission). The DC motor driving the wheel can take care of all vehicle speed changes. Based on the storage (range) capability of the batteries the vehicle can run in a purely electric mode for certain distances with the IC engine started only when the batteries are almost discharged. A schematic of the series hybrid configuration is shown in figure 1.2.

The advantage of a series hybrid is that the engine runs at its best efficiency, thus generating the maximum electrical energy to charge the battery. Since the engine is constantly operating

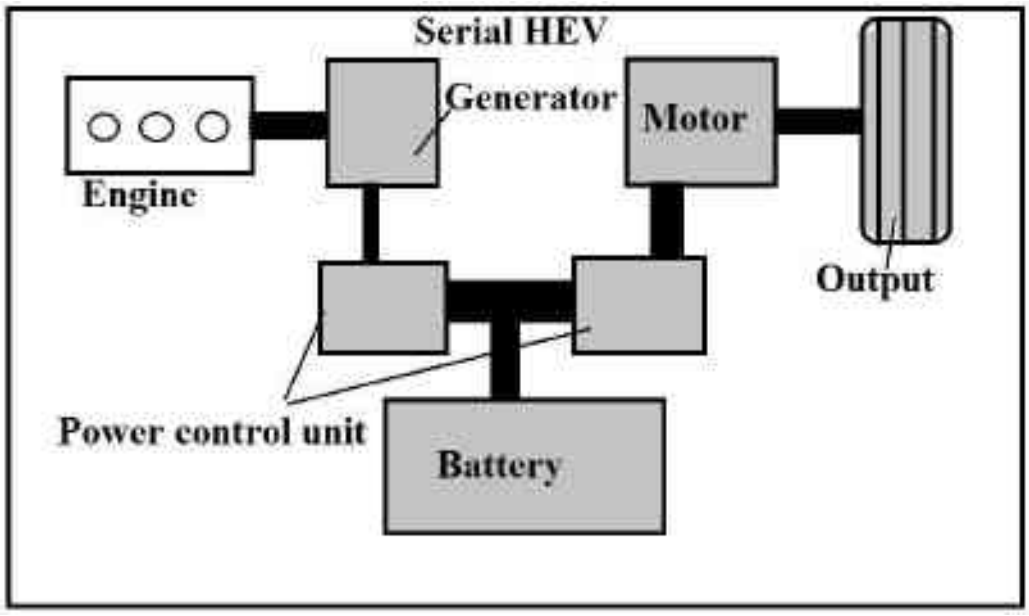

Figure 1.2: Schematic of a series hybrid electric vehicle

at its optimum efficiency, and the vehicle receives its power solely from the electric motor, this system is most efficient during the stop and go city driving. In addition, the internal combustion engine of the series hybrid vehicle can be replaced by a fuel cell, thus converting it into a pure electric vehicle. The main disadvantage of the series hybrid also results from its architecture – the IC engine, the generator, the batteries and the electric motor must all be designed to meet peak power requirements! In other words, for a desired power of say X kW from the vehicle, the IC engine must be able to produce X kW, the generator and batteries must be capable of giving the equivalent of X kW and the electric motor must also be capable of delivering kW. One can clearly see that all the equipments in the power train must be designed to meet the desired peak load and this makes the entire system expensive.

Power split

In this architecture, a planetary gear set or PGT[1] is used to transmit power from the engine to the wheel axles. This allows engine speed to be decoupled, to some extent, from vehicle speed . The PGT enables the engine power to flow to the wheel and the engine power can also flow to an electric generator, producing electricity that in turn supplies power to the motor to propel the wheels. Often a number of batteries can also be placed in between the generator and the wheel and this can supply power to the wheel for very short periods as in the Toyota Prius.

[1]Another approach would be to use a continuously variable transmission or CVT (see figure 4.7).

Hence, the power split system allows both 'parallel like' and 'series engine like' operations to be combined to some extent.

1.2 Hybrid electric energy management process

In general, the main reason for using a hybrid electric architecture is to efficiently use the available electric motor and the IC engine for improved fuel economy, reducing emissions and/or increased power at the wheel when required. The combination provides the necessary extra degree of freedom, at each instant of time, since the power needed by the vehicle can be provided by either one of these sources, or by a combination of the two. In this section, we present various approaches for the control ands management of the two available power sources to achieve optimal fuel efficiency and other requirements of the vehicle.

Choosing the correct combination of power sources is usually a complex problem. If the vehicle is decelerating, it is obvious that the energy storage system (i.e. battery) should receive as much of the braking energy as possible and the rest is dispersed using mechanical braking. However, if the vehicle is accelerating, it may be more advantageous to use the engine and leave the battery charged for later use, or to use some of the energy stored in the battery instead of running the engine. In general, the answer to this question depends on several variables. The first aspect to consider is the actual objective of hybridization. In general, it is possible to define the objective of hybridization as the minimization of a given cost function, representing fuel consumption, emissions, or a sum of both. The minimization should ideally take place over the entire life cycle of the vehicle, but in practical cases the optimization horizon is limited to a short trip or section of a trip, with duration of several minutes or a few hours.

The other important issue to be taken into account is the type of hybrid vehicle. In particular, a charge-sustaining vehicle will be characterized by the fact that the state of charge of the electric storage system (e.g. battery) at the end of the optimization horizon should be the same or close to as it was at the beginning. In this case, the entire energy needed for completing the trip derives from the fuel. A charge-depleting, or plug-in, hybrid vehicle instead uses its batteries much more, and the state of charge can decrease sensibly at the end of a trip, because the vehicle can be plugged in the electrical grid to be recharged. In this case, a substantial amount of the total energy needed for a trip is deriving from the battery (and ultimately from the electric grid), not the fuel. The differences between the two cases, in terms of the control problem, can be seen as different final conditions and different optimization objectives. Final conditions are different because the state of charge variation is zero for charge-sustaining

hybrids, but can be arbitrary or pre-determined for plug-in hybrids. The difference in optimization objectives is that,while fuel consumption is generally the minimization objective in a charge-sustaining hybrid, the total energy consumption, or the total expense, may be a more signicant cost function for a plug-in vehicle [9].

In general, once a suitable optimization horizon and cost function have been decided, the control problem in hybrid vehicles consists in minimizing the total cost (an integral function) using a sequence of instantaneous actions. This is a typical optimal control problem, and several methods can be used for its solution. In this section, we attempt at an informal description of the possible approaches. These can be subdivided into four categories:

- Numerical optimization
- Analytical optimal control theory
- Instantaneous optimization
- Heuristic control techniques

In the first two cases, the problem is considered along the whole time line, i.e. taking into account at each instant information related to past, present, and future time; in the latter two, the solution at each time is calculated based only on current information

Numerical optimization

In general, the optimal solution to the problem is only achievable if the entire horizon is considered at once, i.e., if the driving cycle is well defined and known in advance. This is clearly not possible in a real world application, because it is impossible to know the exact driving conditions (speed, road slope etc.)of the vehicle in advance, or even the duration of the trip. Despite this, obtaining the ideal case in which perfect information of the entire trip is available is a interesting case. Even if not directly applicable, the optimal solution obtained in simulation can be used as a comparative benchmark for implementable strategies, and to gain insights into the behavior of the system. The method most widely used for obtaining the optimal solution in case of perfect and complete information is dynamic programming [10, 11, 12], which is a numerical technique for solving the optimal control problem backwards in time, i.e., starting from the final instant of the driving cycle and proceeding backwards, ending at the initial time. It is based on Bellmans principle of optimality [13], stating that, given an optimal control sequence for a problem, the optimal sequence from any of its intermediate steps to the end corresponds to the terminal part of the overall optimal sequence. Based on Bellman's principle

of optimality, the optimal solution can be calculated step by step starting at the final time and minimizing the cost-to-go at each step, i.e., the cost incurred in moving from that step to the end. From a practical standpoint, dynamic programming gives the same results that would be obtained considering all the possible combinations of control sequences and choosing the one with the lowest total cost, but in a fraction of the computational time, because the number of combinations to be evaluated is greatly reduced. In fact, at each time step the optimal path to the end is found and stored, discarding all the other combinations, because the optimality principle guarantees that the solution from there to the end will not be affected by the previous control actions.

Analytical optimal control theory

Traditional optimal control theory in existence since the 17th century [14] provides a mathematical framework for addressing the dynamic optimization problem. However, the energy management problem in hybrid vehicles is very complex and must be simplified and abstracted significantly in order to be completely solved using these analytical techniques. Nonetheless, applying optimal control theory to the simplified problem allows for its better understanding and the results obtained can further improve the practically implementable solutions on hybrid vehicle. One of the most important approach in optimal control theory is the use of Pontryagins minimum principle [15, 16, 17]. This approach gives necessary condition that the optimal solution must satisfy. Despite offering only necessary optimality conditions, the principle is useful because it can, in principle, be applied to any problem since it does not impose any restrictive hypothesis on the analytical properties of the mathematical functions involved in the problem formulation. In practice, Pontryagins principle can be used to generate solution candidates. If the optimal control problem admits one solution and the necessary conditions are satisfied by a single candidate, the solution obtained with this principle is an optimal solution.

In the field of hybrid electric vehicle optimization, Pontryagins principle has been used by several authors [18, 19, 20] to find the optimal power split given the driving cycle. It can be a valid alternative to dynamic programming if the powertrain can be described with simple analytical functions. In practice, it cannot be applied without a-prior knowledge of the drive cycle although it can provide insights into the problem.

Instantaneous optimization

A third family of control strategies includes those that modify the global optimal control problem into a sequence of local instantaneous problems, thus calculating the solution as a sequence

of local minima. This approach works well if the local minimization is well defined. The equivalent consumption minimization strategy (ECMS), first introduced by Paganelli et al. [21], is the most well-known of these strategies. ECMS especially in charge-sustaining vehicles is based on the assumption that the difference between the initial and final state of charge of the battery is zero or negligible with respect to the total energy used. This implies that the electrical energy storage is used only as a buffer. Since all the energy finally comes from fuel, the battery can be seen as an energy storage system. The electricity used during a battery discharge phase must be replenished at a later stage using the fuel from the engine (either directly or indirectly through a regenerative path). Possible cases at a given operating point:

- The battery power is positive (discharge case): The battery is recharged with the engine which results in additional fuel consumption in later stages.
- The battery power is negative (charge case): the stored electrical energy will be used to reduce the engine load, which implies a fuel saving.

The instantaneous cost that is minimized at each instant is called equivalent fuel consumption and is obtained by adding a term to the actual engine fuel consumption. This term is positive in case 1 above and negative in case 2. It represents the equivalent fuel consumption associated with the use of the battery and a solution close to optimality is obtained by proper definition of equivalent fuel consumption, while maintaining the battery state of charge at the desired level. The major advantage of this approach, based on instantaneous minimization, is that it easily implementable in real time. As mentioned, a proper definition of the equivalent fuel consumption is necessary to achieve quasi-optimal results and this requires optimization of the tuning parameters which is only possible if the driving cycle is known in advance. Good results have also been achieved with adaptive ECMS based on driving pattern recognition [22]. Adaptive ECMS is a more refined strategy that can recognize the type of driving conditions in which the vehicle is being used (e.g. city, highway, suburban roads etc.) and it dynamically adapt the definition of virtual fuel consumption in order to find the best match to each driving pattern.

Heuristic control techniques

Heuristic control techniques are not based on minimization or optimization, but rather on a pre-defined set of rules. The rules generate the control action based on the instantaneous values of several significant vehicle parameters. Most of the time, rules are derived using engineering knowledge and a substantial amount of testing for arriving at the optimum control parameters

[23, 24, 25]; the technique can be made robust and suitable for production vehicles, but the results may not be optimal, since they are not based on formal optimization techniques. In some cases rules can be extracted from the optimal solution found using dynamic programming, thus representing a method to implement the optimal solution. For example, it may be possible to create a set of rules that try to follow the optimal vehicle behavior based on the observation of external inputs and the state of the system [26, 27].

1.3 Motivation and scope

As mentioned, a hybrid electric vehicle uses two or more power sources, usually an internal combustion engine and an electric machine. It combines the range advantage of a conventional vehicle with the environmental benefits of an electric vehicle while retaining the performance levels [28]. The pragmatic approach towards development of next generation urban vehicles, with high fuel efficiency, low or zero emissions and compact design to negotiate crowded roads, involve use of hybrids (see, for example [29, 30, 31], and the references contained therein). In India, studies show that 80% of the growth in the personal transport segment is expected for small cars, in particular in the so-called A & B segments. In India and a few other Asian countries, a three-wheeled vehicle called an auto-rickshaw is one of the most affordable and convenient form of public (for hire) transportation. The popularity is primarily due to the low-cost with minimal features, reasonable fuel efficiency and the small size and narrow body making them perfectly suited for navigating the narrow and heavily congested roads of Indian cities and urban environment. These vehicles are usually powered by a two- or four-stroke gasoline engine and as can be readily seen in Indian roads, they are typically highly polluting (see also [32]). Due to traffic and congestion, in a typical travel there are extensive start-stop cycles, the speeds are low and they have a typical range of about 120 km. These and various other reasons make the three-wheeled auto-rickshaw an eminently suitable candidate for conversion to hybrid architecture.

The proposed three wheeled parallel hybrid electric vehicle (HEV) is based on the very commonly seen Bajaj auto-rickshaw. The detailed specifications and usage pattern of this vehicle are available in reference [33]; we present them here for completeness. The Bajaj auto-rickshaw comes with a 2/4 stroke IC engine. The vehicle specifications given in table 1.1.
The geometry of the above vehicle is given below:

Table 1.1: Geometry of auto-rickshaw

Parameter	Value
Length	2675 mm
Width	1240 mm
Height	1690 mm
Clearance	200 mm
Frontal area	2.09 m^2
Coeff. of drag	0.5
Center of vehicle mass	0.4 m
Wheel base	1.075 m

The engine is suitable for the load of 4 persons including the driver which is the primary application of the vehicle and the specifications of the engine are given in table 1.2
The engine specifications are as follows:

Table 1.2: Engine specification of auto-rickshaw

Parameter	Value
Type	Four stroke, SI, air cooled
Weight	45 Kg
No. of cylinders	one
Displacement	173.52cc
Max. power	6KW@5000 rpm
Max. torque	12.7Nm@4000 rpm
Max. payload	310 Kg

Before a hybrid three-wheeled auto-rickshaw could be built, modeling, simulation and experiments are needed. In this work, we first create models of a hybrid auto-rickshaw with a novel hybrid architecture. Simulations are conducted on the Indian Driving Cycle to obtain fuel efficiency and comparison are made with traditional hybrid configuration. Using dynamic programing, algorithms are developed for efficient energy management. Finally, a test bed consisting of an auto-rickshaw IC engine, a DC hub motor and batteries is developed and experiment with various hybrid architectures were done.

1.4 Contributions of the thesis

The main contribution of this thesis are as follows:

- Collecting and analyzing the actual usage pattern of auto-rickshaws in the city of Bangalore, Karnataka, India with the help of GPS tracking systems.
- Proposing a novel hybrid propulsion architecture which uses speed addition to combine both the power sources at the output instead of conventionally used torque addition which requires complex powertrains.
- Modeling and simulations using MATALB/Simulink of the proposed hybrid architecture and comparison of the speed addition with typical torque addition using heuristic control.
- Modeling and simulation of speed addition and torque addition configuration using MATLAB/Simulink by applying optimal control algorithm using dynamic programming for benchmarking the fuel consumption of both the configurations.
- Design and fabrication of a test bed for a novel parallel hybrid configuration consisting of DC hub motors and an IC engine.
- Obtaining experimental data and comparing with conventional torque addition parallel hybrid. Experimental results clearly shows the addition of speeds and thus serves as a proof-of-concept of the novel hybrid system.

1.5 Preview

The thesis is organized as follows: in Chapter 2, we present the data collected from movement of auto-rickshaw in traffic and also show the approach used in modeling various components of powertrain. In Chapter 3, the difference in torque addition and speed addition is described using a rule based control and an in-depth discussion of dynamic control and its application to current model gives the fuel consumption and various other characteristics of both the configurations. Chapter 4 describes the test bed used for experimental validation of the system and presents experimental results for speed and torque addition configurations. Finally in Chapter 5 we present the conclusions and present the scope for future work in this area.

Chapter 2

Modeling of an hybrid electric vehicle

Essentially, all models are wrong, but some are useful -George E. P. Box

2.1 Introduction

Any mathematical model of a system is an approximation of the physical reality. To create an useful model, it is necessary to understand what level of approximation is acceptable for the application in focus and then to identify suitable mathematical models capable of delivering the right compromise between complexity, computational time and accuracy. A good model is still not perfect replication of physical system, but it can be useful if its limits and assumption are known, they are appropriate for its application and produces the results close to the actual system.

In this chapter, we discuss the modeling of a vehicle with a primary objective to evaluate fuel consumption based on how the energy flows in vehicle powertrain, identifying the source of losses and respective efficiencies of subsystems. We first present the data collected and the statistics on the movement of auto-rickshaws in Bangalore, India. Then we present a brief overview of the methods typically used to evaluate fuel consumption in conventional and hybrid vehicles and describe the approach used in this work. Finally we present the proposed concept of speed addition configuration and compare with that of a conventional torque addition configuration.

2.2 Auto-rickshaw usage in Bangalore

In this Section, we present the details of the sample usage data of three-wheeled auto-rickshaws in the city of Bangalore, India. The data was collected from four auto-rickshaws over a period of 30 days each in late 2010 and early 2011. The number of vehicles and congestion has increased significantly in the last five years and this has probably resulted in slower speeds and more

start-stop operations.

2.2.1 GPS based data logging for auto-rickshaw usage

To collect actual usage data, we acquired 4 DG-100 GPS data logger systems from GlobalSat Technology Corporation [34]. These were given to 4 auto-rickshaw drivers who would carry these data loggers with them during their normal daily plying on the streets of Bangalore, India. After their shift, the data would be downloaded to a laptop and data recorders given back to them for the next day. The drivers collected data over approximately 30 days each.

A typical data set contains data about date, time, latitude, longitude, and speed. The data collection frequency can be set and we had chosen to collect data every 30 seconds and for this setting the 95 data points are stored in an interval. Figure 2.1 shows the data collected on day by driver #2 during one such interval starting from approximately 11:27 am to 12:15 pm on November 16, 2010. The data stored in this interval can be seen on Google Maps as shown in figure 2.1. According to the data obtained from the data logger, there are 15 such intervals

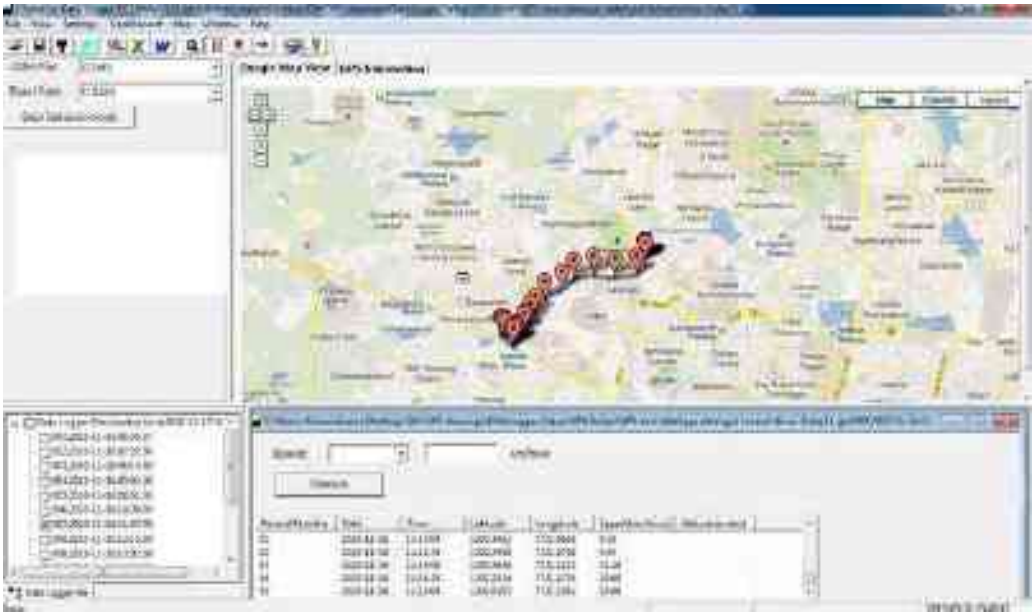

Figure 2.1: A typical interval in data collected by the GPS data logger

for day 11 starting from about 6:30 am to about 6:30 pm. The last recorded interval is shown in figure 2.2 below.

2.2.2 Analysis of usage data

The data collected was analyzed using Matlab and several useful quantities could be recovered from the collected data. One of the important data that could be easily obtained is the distri-

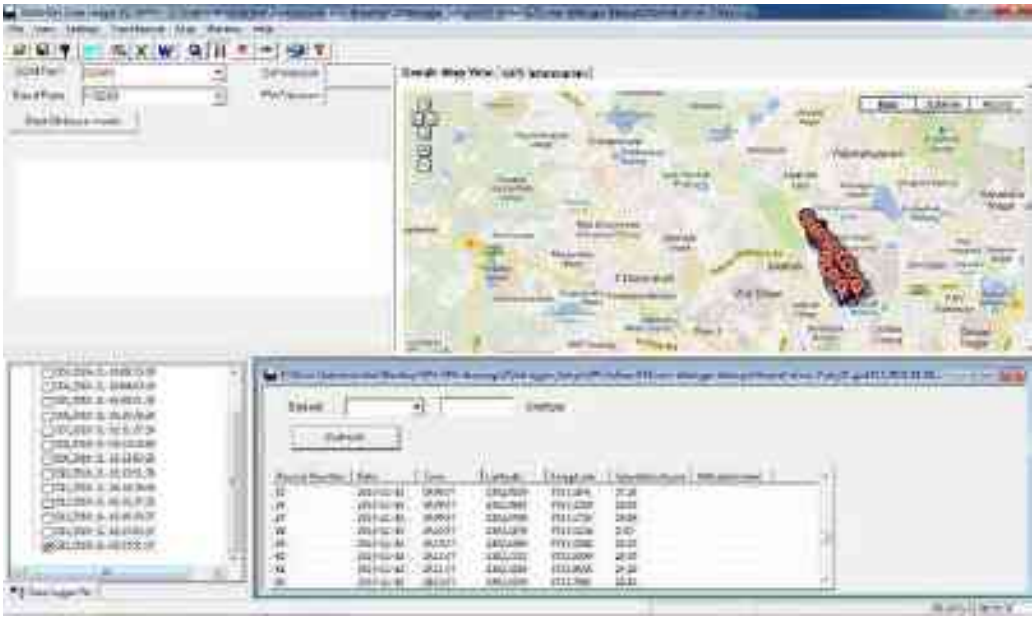

Figure 2.2: Data from data logger for interval 15 on day 11

bution of vehicle speed. Figure 2.3 shows the distribution of the speed of the auto-rickshaw for Driver 1 on day 11. One can observe that on this particular day, the vehicle was stationary for more than 50 % of the 12 hour working period. Additionally, the vehicle was traveling between 0 and 5 km/h for about 7 % of the time and more than 75 % of the time the vehicle speed was less than 20 km/h. The maximum speed of the vehicle was approximately 50 km/h. It may be noted that a stationary vehicle does not mean the vehicle was stuck in traffic or at stop signs in the road more than 50 % of the time – it also includes rest periods and breaks taken by the driver. Typically an auto-rickshaw driver would be crawling at low speeds when he does not have a passenger and he is on the lookout for one. The 7 % of the time period spent between 0 and 5 km/h may not be due entirely to traffic congestion and a large part could be due to the driving pattern when the driver is looking out for passengers.

Similar data collected from other drivers on different days is shown in figures 2.4, 2.5 and 2.6. It can be seen that the vehicle consistently remains stationary for more than 50% of the time irrespective of the path or the driving habits. The vehicle speeds vary slightly based on the traffic conditions, route taken by the driver and driving habit of the driver.

The GPS data also tells us the distance traveled by the auto-rickshaw in a typical working period of 12 hours. For the day 11, whose speed distribution is shown in figure 2.3 the total distance traveled was 105 km. Similarly distance traveled on other days could be found out. Figure 2.7 shows a sample of distance traveled by the same driver in 9 days.

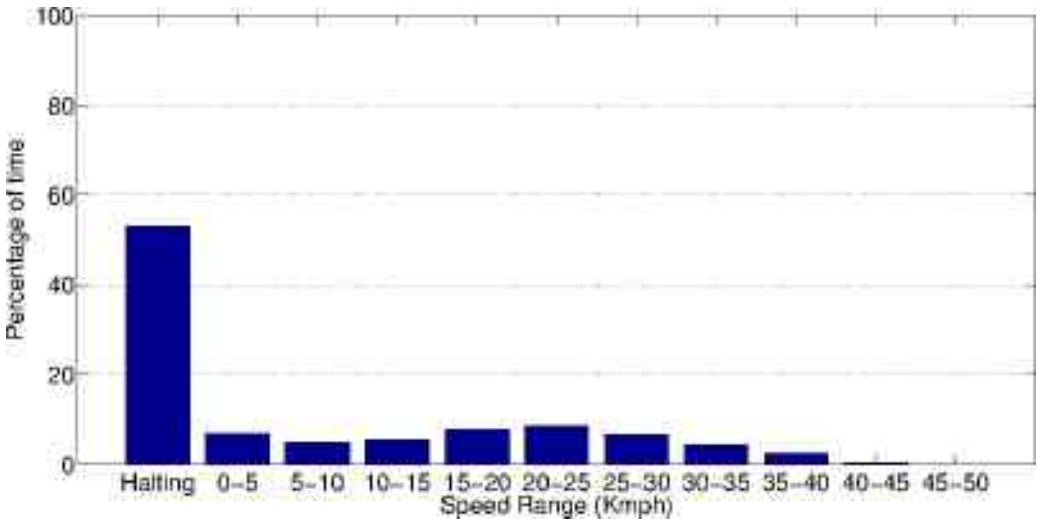

Figure 2.3: Speed distribution of driver 1 on day 11

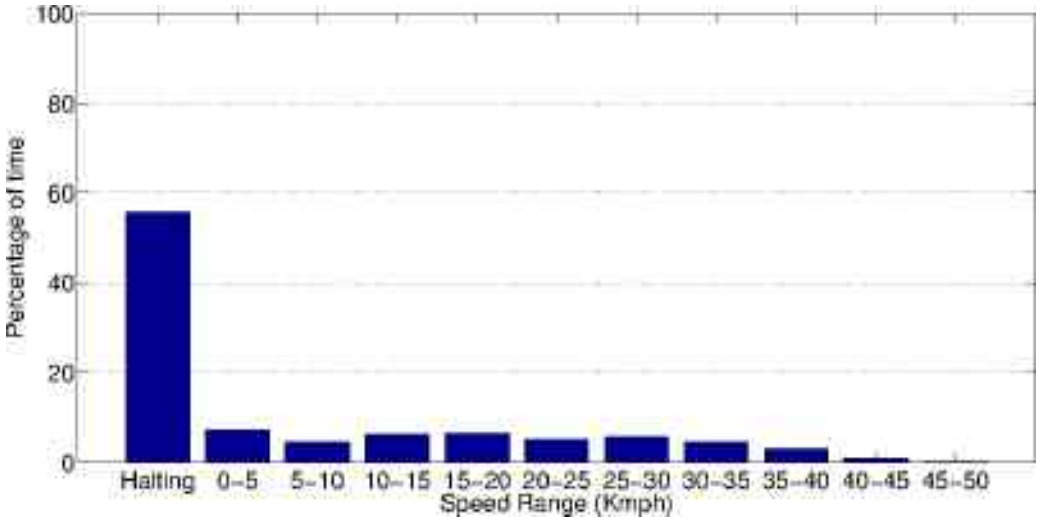

Figure 2.4: Speed distribution of driver 2 on day 18

As mentioned earlier four drivers collected data for a period of 30 days each. Although, the sample is small and more data is required, the statistical analysis of the collected data was performed. The key statistics of the collected data are as follows:

- Mean speed: 12.5 km/h
- Standard deviation of speed: 11.8 km/h
- Maximum speed: 62 km/h
- Minimum and maximum distance in a single day: 8.6 km and 137.6 km, respectively

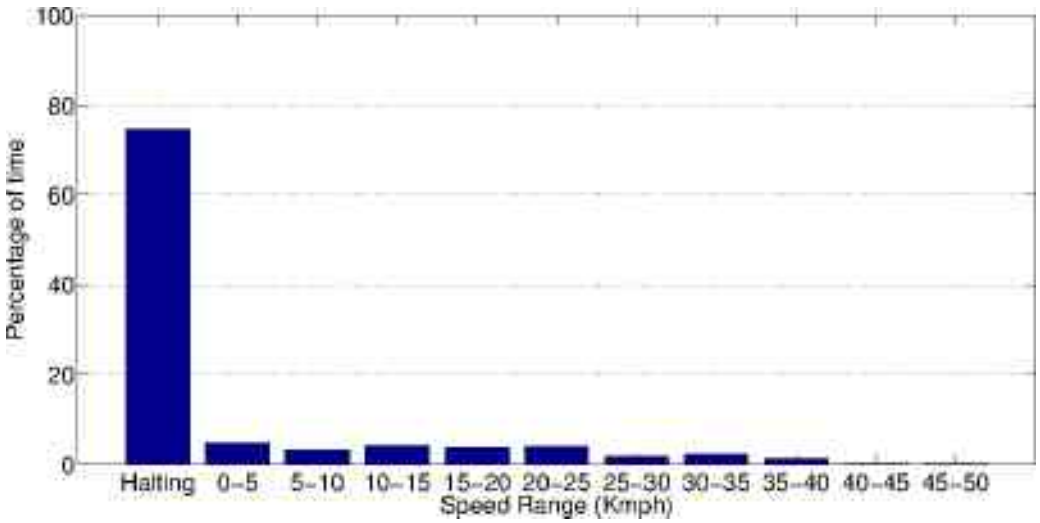

Figure 2.5: Speed distribution of driver 3 on day 15

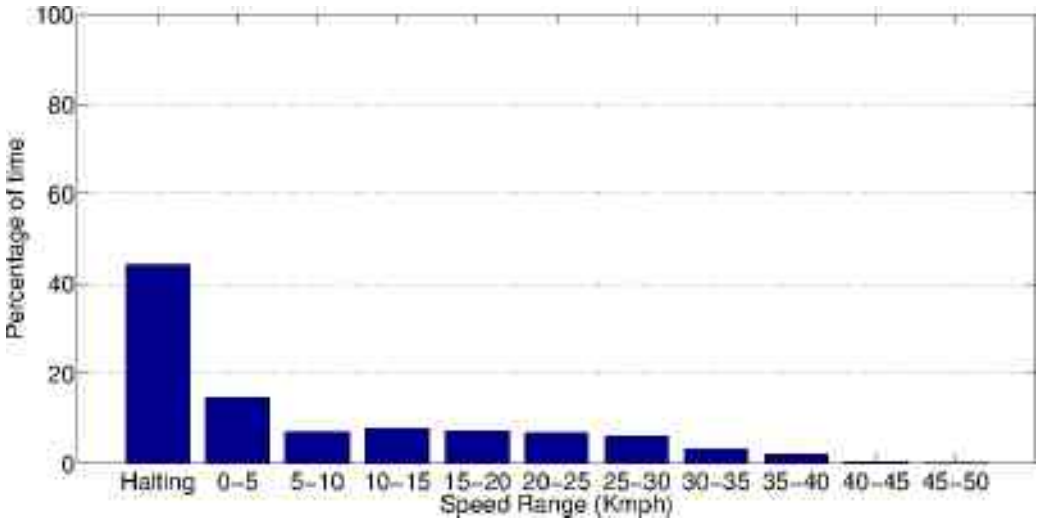

Figure 2.6: Speed distribution of driver 4 on day 2

- Mean distance and standard deviation: 72.6 km and 28.4 km, respectively.

An analysis of the usage data also reveals that between 35 and 60% of the time the vehicle is either stationary or crawling at speeds less that 5 km/h. Further data collection is required to determine variation in speeds with time of day and location in the city. Likewise more data is required to obtain more reliable statistics on auto-rickshaw usage in other urban areas.

In summary we can conclude from the data from four auto-rickshaws that the typical speeds are very low, the range is of the order of 120 km and there are significant numbers of start-stop

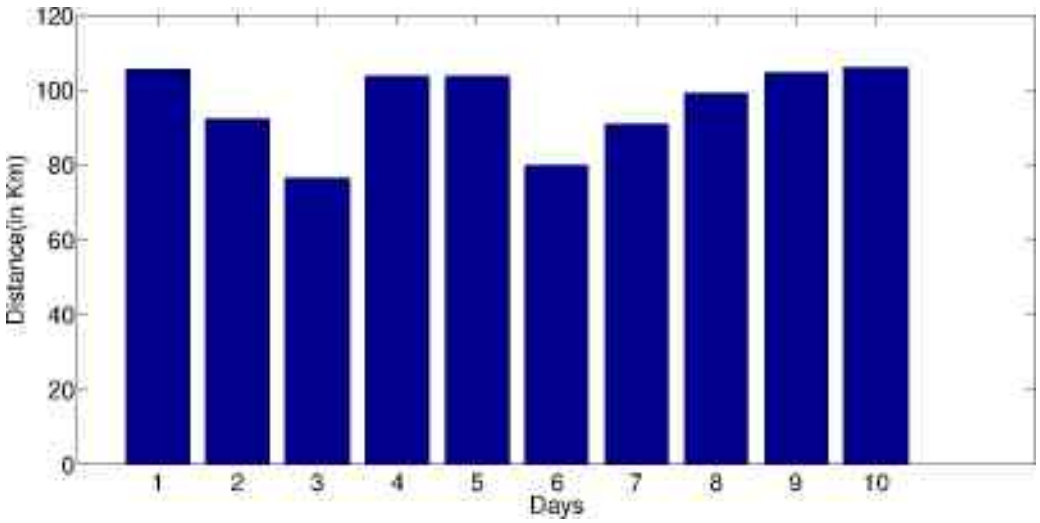

Figure 2.7: Distance travelled by auto-rickshaw on various days

cycles[1]. From the data, it is clear that the three-wheeled auto-rickshaw is a good candidate for possible conversion to hybrid propulsion. With parallel hybrid architecture and the vehicle being operated for a large time in the pure electric mode, a significant increase in fuel economy and decrease in pollution can be expected.

2.3 Modeling of a vehicle for fuel efficiency

A vehicle consisting of thousands of components, is a complex system. A great amount of literature exists in the field [35, 36, 37]. In this section the primarily goal is to obtain reasonably accurate model to estimate fuel efficiency and to derive this model using general principles of mechanics. In order to evaluate fuel consumption, we first describe the energy flows in a vehicle powertrain, identifying the source of losses and describing the relevance of driving cycles in the energy balance. Then we present a brief overview of the methods normally used to evaluate fuel consumption in conventional and hybrid vehicles, and finally describe the models used in this work and their implementation.

2.3.1 Forces acting on a vehicle

The available mechanical energy from burning of fuel in an IC engine is consumed to accelerate the vehicle, over road and aerodynamic resistance and to move on a grade. Assuming the

[1]Not presented in this work, but data collected when traveling on city buss and in private cars, the slow average speed and large number of start-stop cycles are also clearly visible.

vehicle to be a point mass, the force equilibrium equation can be written as:

$$M_{\text{vehicle}}\frac{dV_{\text{vehicle}}}{dt} = F_{\text{traction}} - (F_{\text{roll}} + F_{\text{aero}} + F_{\text{grade}}) \tag{2.1}$$

where M_{vehicle} is the total vehicle mass, V_{vehicle} is the vehicle velocity, F_{traction} is the tractive force generated by the powertrain at the wheels, F_{roll} is the rolling resistance and F_{aero} the aerodynamic resistance, F_{grade} the force due to road slope.

Each of the terms in the bracket on the right-hand side are discussed in detail next.

Rolling resistance

The rolling resistance of tires on hard surfaces is primarily caused by hysteresis in tire materials. Rolling resistance is defined by the National Academy of Sciences as ''A characteristic of a deformable material such that the energy of deformation is greater than the energy of recovery ... as the tire rotates under the weight of the vehicle, it experiences repeated cycles of deformation and recovery, and it dissipates the hysteresis energy loss as heat .... the main cause of energy loss associated with rolling resistance and is attributed to the viscoelastic characteristics of the rubber" [38]. Rolling resistance is mainly due to the hysteresis in deformation of rubber material. The hysteresis of rubber material results in the shift of reaction force which is generally aligned with the weight of the vehicle – figure 2.8 shows the shift in reaction force by a magnitude of a. To keep the vehicle moving [39], we have

$$F_{\text{roll}} = \frac{Pa}{r_d}F_{\text{roll}} = f_{\text{rmg}} \tag{2.2}$$

where m is the mass of the vehicle, g is the gravitation acceleration and f_r is the rolling friction coefficient.

Aerodynamic resistance

Drag is the force of wind or air resistance pushing in the opposite direction to the motion of the vehicle. The two types of aerodynamic drag that act against a vehicle are shape drag and skin friction drag.

Shape drag: The forward motion of the vehicle is opposed by the air in front of it. Since, the air cannot instantaneously move out of the way and its pressure is thus increased, resulting in high air pressure opposing the motion of the vehicle. In addition to opposing force, the air behind the vehicle cannot instantaneously fill the space left by the forward motion of the vehicle and a zone of low air pressure is created at the back resulting in a backward pull. These two

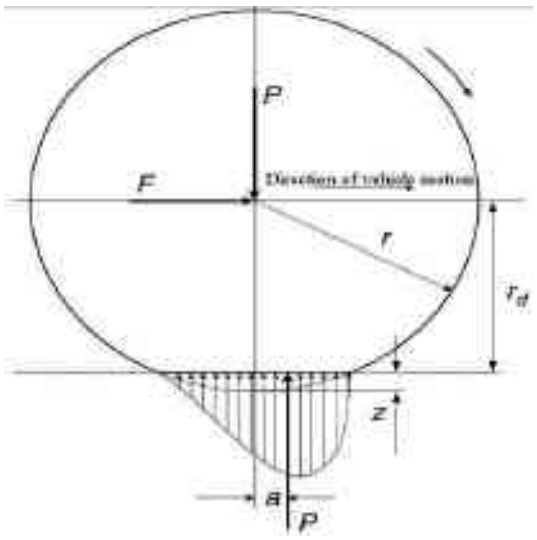

Figure 2.8: Tire deflection and rolling resistance of tire on road

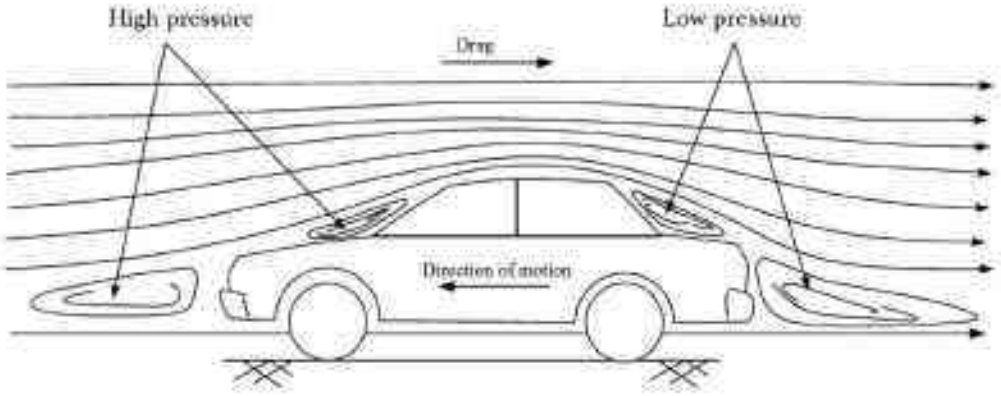

Figure 2.9: Drag forces acting on vehicle due to shape of the vehicle.

zones of pressure oppose the motion of the and the resulting opposing force on the vehicle is the shape drag.

Skin friction: The air close to the vehicle surface moves almost at the speed of the vehicle while air away from the vehicle remains still. The difference in the speed produces a friction that results, in the second component of aerodynamic drag.

Aerodynamic drag is a function of vehicle speed, vehicle frontal area, shape of the vehicle

and air density [40]. It can be modeled as

$$F_{\text{aero}} = \frac{1}{2}\rho A C_D (V - V_w)^2 \tag{2.3}$$

where C_D is the aerodynamic drag coefficient that characterizes the shape of the vehicle body, A represents the vehicle frontal area, ρ represents air density, V is the vehicle velocity and V_w is component of the wind speed along the vehicle moving direction. We assume the air is standstill. Hence the aerodynamic drag is given by

$$F_{\text{aero}} = \frac{1}{2}\rho A C_D V^2 \tag{2.4}$$

Grade resistance

When the vehicle goes up the slope the horizontal component of the vehicle mass acts against the motion of the vehicle. This can be observed from the figure 2.10. The grade resistance component of vehicle energy balance is given by equation (2.5)

$$F_{\text{grade}} = Mg \sin\alpha \tag{2.5}$$

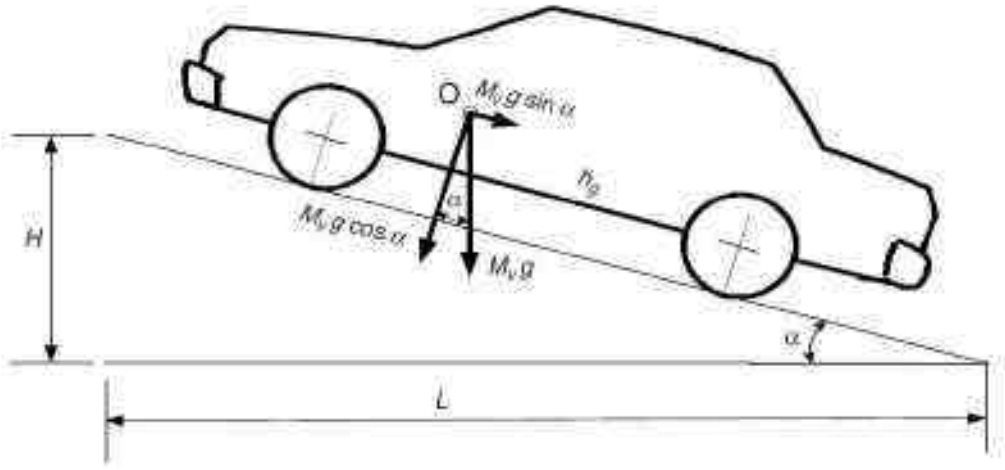

Figure 2.10: Vehicle on an inclined slope

2.3.2 Internal combustion engine

There exists sophisticated models for IC Engines in literature [41, 42, 43]. For our purpose of estimating fuel efficiency, the IC engine model is a static model which neglects engine dynamics and torque oscillations. The developed engine torque is applied to the crankshaft and flywheel

lumped together in a single rotational inertia. The engine is also subject to the load torque coming from the rest of the powertrain or the mechanical interface between the IC engine and the wheel. For any engine, a table of torque, speed and fuel consumption is generated from static load tests and we assume that such a table is available – in our case, such a table also known as the engine map for an 175 cc engine was available[1] and this was used in this study. A plot of fuel efficiency of the IC engine is shown in figure 2.11 and the numerical values are available in Appendix A.

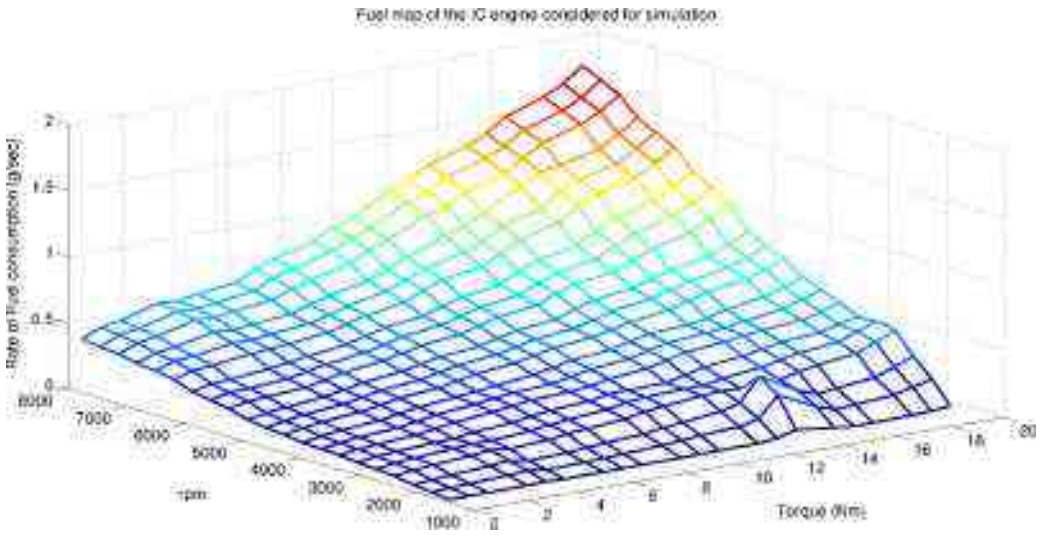

Figure 2.11: Fuel map of IC engine considered in this thesis

To obtain the generated engine torque at a specific speed along the drive cycle, interpolation based on the maximum available torque at the current speed and the percentage acceleration required is used. To obtain fuel consumption again interpolation between nearby torque and speed points is used. The required torque at a specific speed is applied to the equivalent inertia, which represents the crankshaft and the flywheel. It may be noted that torque and fuel consumption is based in the load that is applied to generate the engine map – it does not take into account additional loading due to passengers or goods being transported by any vehicle.

2.3.3 Powertrain components

The torque developed by an engine is transmitted to the wheel using mechanical elements such as gears, clutch, brakes etc. There exists extensive literature on modeling these components. We restrict the discussion and modeling for components used for the proposed hybrid concept we use and for the goal of estimating fuel efficiency.

[1]The engine data was made available from GM R&D, USA.

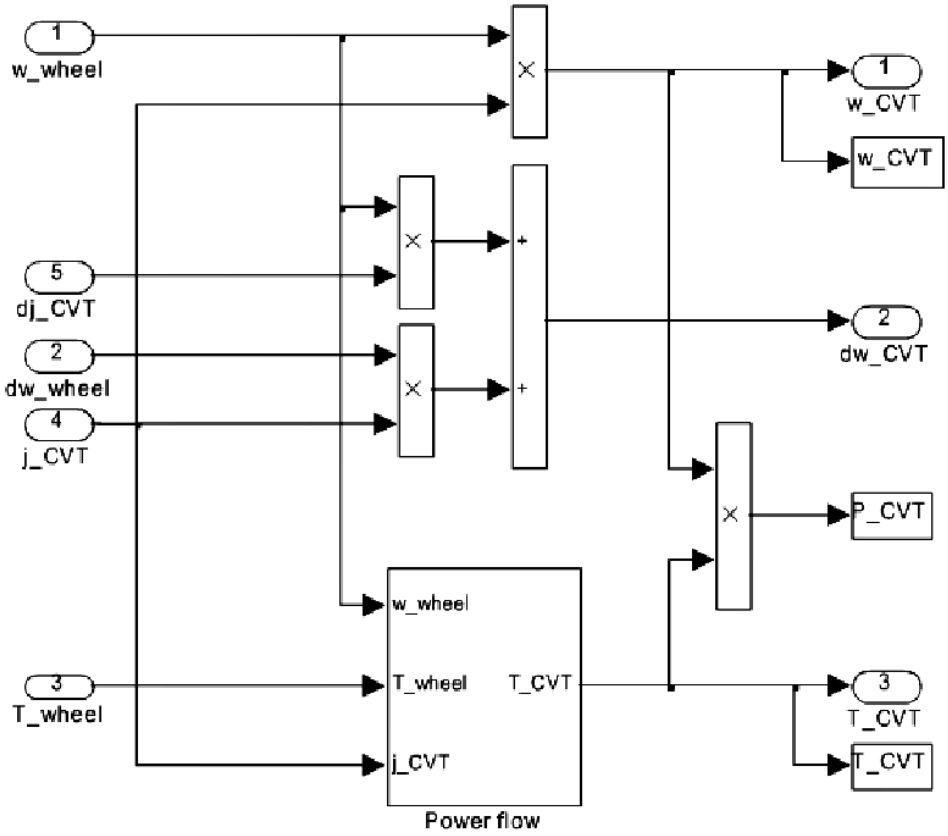

Figure 2.12: CVT simulink model

Continuously variable transmission

A continuously variable transmission (CVT) is like an automatic transmission but without fluid coupling and have reasonably high efficiency when the power required to be transmitted is low (less than 10 HP). Details about CVT theory, design and analysis can be obtained from references [44, 45]. We give a brief description of the working of a CVT and present a design approach for a CVT to be used for the proposed low-cost hybrid propulsion system.

A CVT design based on the belt-ball variator design was considered. The CVT has been modeled based on QSS toolbox [46] and a Matlab/Simulink model of the CVT is shown in figure 2.12. The control of CVTs demands that it be predictive. This is achieved by transmitting the desired speed from the drive cycle in case of torque addition and required rpm in speed addition directly into the control unit. The transmission to the vehicle block is delayed by one step. The gear ratios are modeled based on the instantaneous crankshaft rpm.

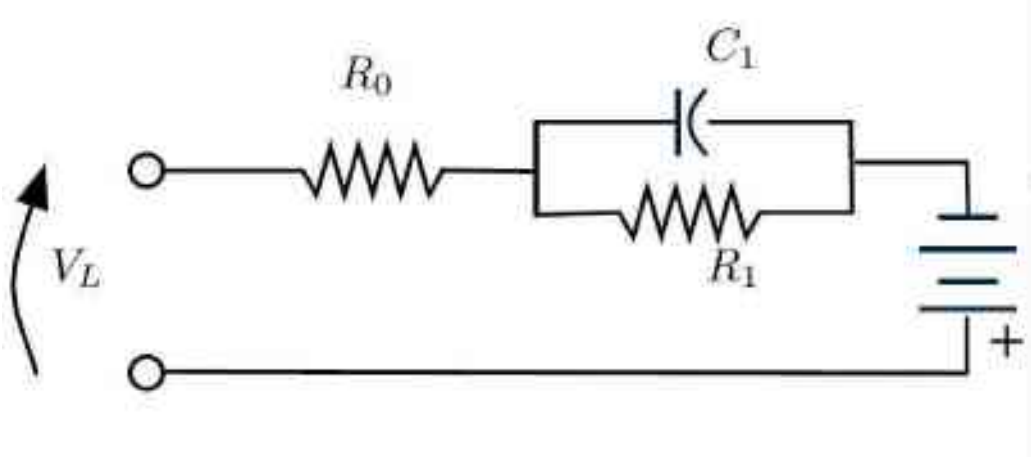

Figure 2.13: Battery circuit model

Energy storage system

Electrical energy storage systems such as batteries and capacitors are key component of all hybrid vehicles. A variety of models have been proposed to evaluate their interaction with the rest of the powertrain. However, for estimating fuel consumption and performance evaluation for a vehicle level, a simple circuit model is sufficient. The simplest dynamic model of a battery is a circuit like the one in figure 2.13.

The series resistance R_0 represents the ohmic losses due to actual resistance of the wires and the electrodes and also to the dissipative phenomena that reduce the net power available at the terminals. The resistance R_1 and the capacitance C_1 are used to model the dynamic response of the battery. This model is a first-order approximation. The values of the parameters are estimated using curve fitting of experimental data, and are generally variable with the operating conditions (temperature, state of charge). Other models of the same kind, with more R-C branches in series, can be used if more accuracy is required. The number of parameters to be identified increases with the model accuracy.

The battery equation is given by [47] in equations (2.6)

$$V_L = V_{OC} - R_0 I - \sum_{i=1}^{n} V_i \tag{2.6}$$

The discharge and charging resistance of the battery is also considered according to the battery specifications. An important issue related to battery usage in hybrid electric vehicles is their aging, due to the aggressive loading cycles to which they are subjected. But, In thesis we don't deal with the concept of battery aging. Battery aging manifest itself as loss of capacity and

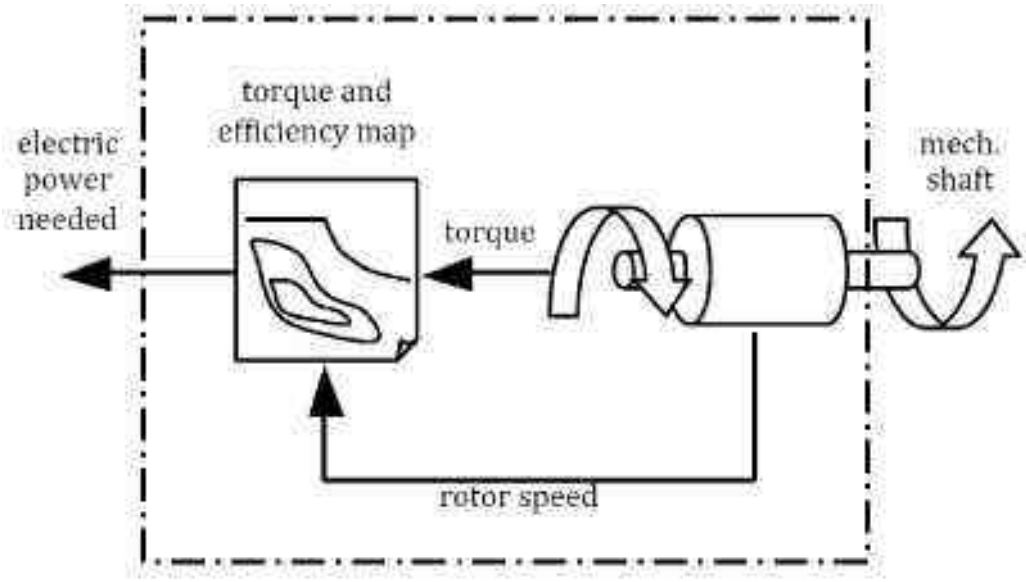

Figure 2.14: Electric motor in traction mode

increase of internal resistance [48], and can reduce vehicle performance. Recent and ongoing research is devoted to determine a suitable model that can predict the amount of residual life given the loading cycles [49].

Electric motor

The conceptual sketch of electric motor model is as shown in figure 2.14. The electric machines are modeled using a system-level approach similar to the one used for the engine, employing maps of torque and efficiency. The rotor inertia is the only dynamic element modeled as the electrical dynamics in any kind of electric machine are much faster. The torque demand is the input and the electric power to meet the required torque input is given by

$$P_{\text{elec}} = \frac{T\omega}{\eta(\omega, T)} \tag{2.7}$$

If the electric motor is used for re-generation, the torque input is negative and results in an electric output based on the efficiency and capacity of the motor.

Wheels, brakes and tires

The wheel represents the link between the powertrain and the external environment. We assume the wheels to be a rolling without slip and the torque applied to the wheel shaft is completely transformed into tractive force. The wheels also convert the longitudinal velocity and load into torque required and angular velocity.

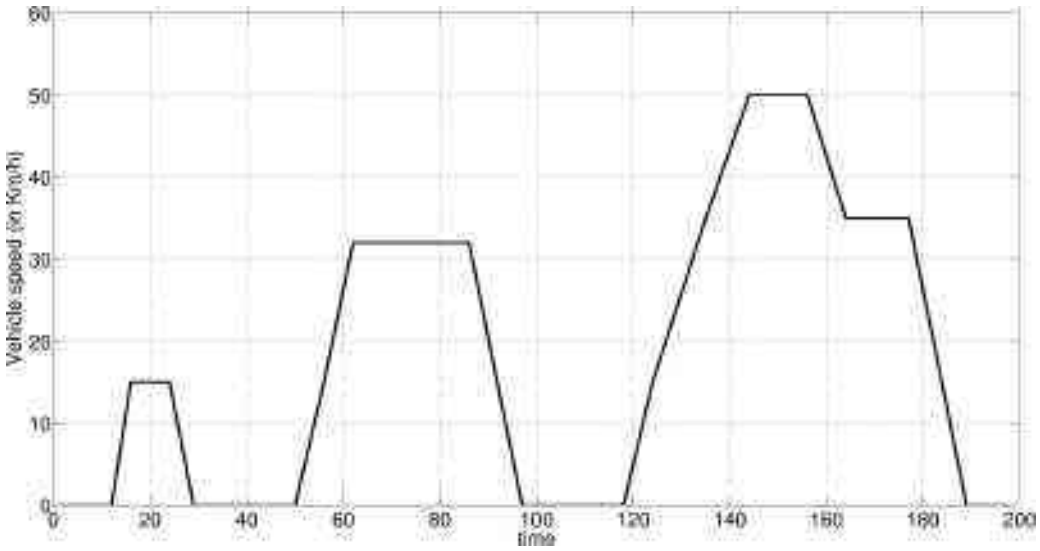

Figure 2.15: Modified Indian drive cycle

2.4 Driving cycle

The performance in terms of fuel efficiency and pollution are obtained for a standard trajectory of a vehicle. This is known as the drive cycle [39]. In this thesis we use a modified Indian Driving Cycle [50]. The driving cycle is similar to the urban driving cycle ECE-15 [51] used in Europe but the top speed is reduced. The details of the modified Indian Driving Cycle are available in the above mentioned reference – we list a few of the important features:

- The modified IDC is composed of 15 phases.
- The duration of one cycle is 195 seconds.
- The peak acceleration is 1.04 m/sec^2 and the maximum cruising speed is 50 km/h.

The plot of velocity versus time according to the modified Indian Driving Cycle is shown in figure 2.15. It can be seen that the actual usage as mentioned in Section 2.2 or as seen in urban driving is very different from the driving cycle for which the performance of a vehicle is estimated.

2.5 Modeling and simulation results

There are three different approaches for modeling of fuel consumption of vehicle for a given prescribed drive cycle [39]. These are

- The average operating point approach

- The quasi-static approach
- The dynamic approach.

The average operating point approach uses a single operating point of the engine, to be assumed as representative of its average efficiency during the driving cycle. The average operating point is calculated starting from the average value of the power request at the wheels during the tractive section of the cycle, and working backwards through the powertrain components. Each component can be represented using its average efficiency.

The quasi-static approach retains the sequential nature of the driving cycle and does not lump all the cycle into a single operating point. It is however based on the assumption that the prescribed driving cycle is followed exactly by the vehicle. The driving cycle is subdivided in small time intervals (typically of 1 s), during which the average operating point approach is applied, assuming that speed, torque, and acceleration remain constant. Each power train component is modeled using an efficiency map, a power loss map or a fuel consumption map. These give a relation between the losses in the component and the present operating conditions, averaged during the desired time interval.

The dynamic approach uses all the dynamic equations of all the sub-components and requires that the state of all the sub-components be available. The modeling of each component can be as detailed as required. This approach is the most efficient approach. However, modeling and obtaining dynamic equations of each component is a difficult process.

The quasi-static and dynamic approaches in-turn can be modeled in two different approaches for modeling based on the information flow. These are the forward and backward simulation. The forward approach is the option typically chosen in most simulators and is characterized by the information flow as shown in figure 2.16. The desired speed (from the drive cycle) is compared to the actual vehicle speed and braking or throttle commands are generated using a driver model (typically a PID speed controller) in order to follow the imposed vehicle trajectory profile. This driver command is an input to the engine and the rest of the powertrain components, which ultimately produce a tractive force. Finally, the force is applied to the vehicle dynamics model, where the acceleration is determined taking into account the road load information [52].

In this thesis, we use the quasi-static approach for estimating the fuel consumption of the vehicle. The drive cycle is divided into 1 second intervals. The average operating point of the vehicle is obtained based the required speed and torque of the vehicle during that time [53]. The IC engine is modeled using the fuel consumption map as described in section 2.3.3. Using the equations (2.1), (2.2), (2.4), (2.5) , the parameters given in Table 1.1, 1.2 and the speeds as

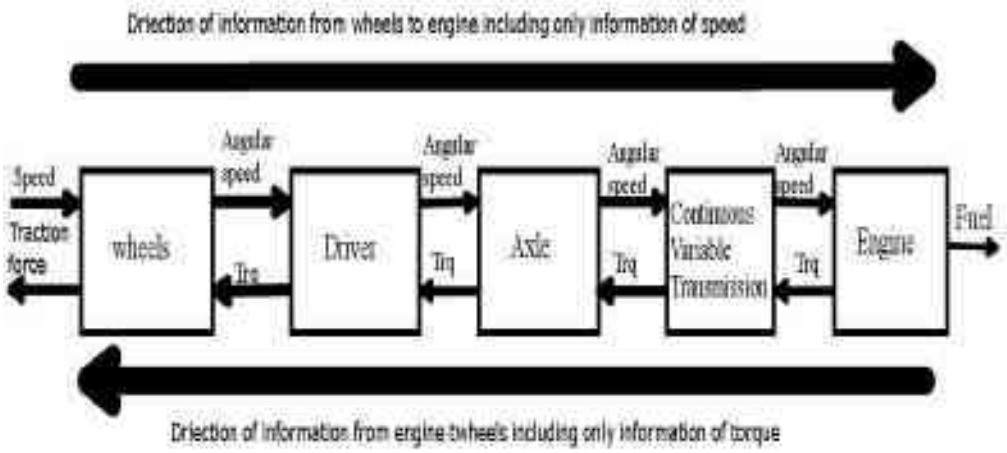

Figure 2.16: Information flow in forward simulation

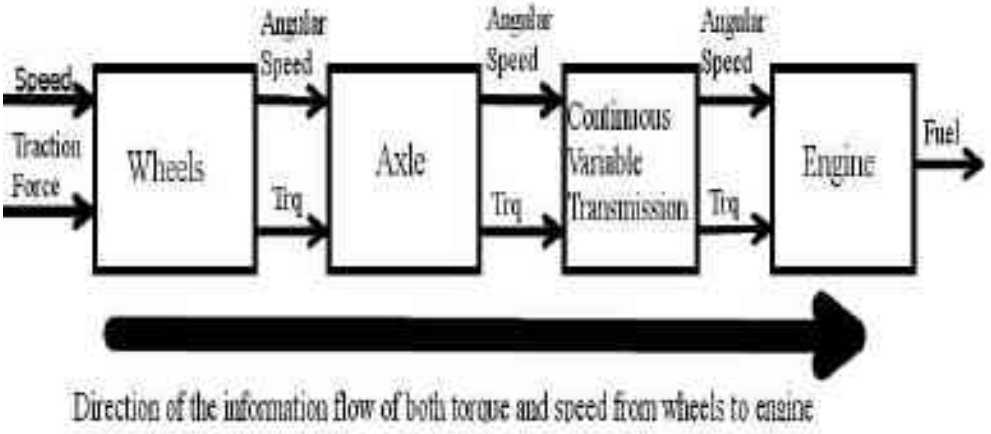

Figure 2.17: Information flow in backward simulation

given in the modified Indian Driving Cycle, the power required to run the vehicle is obtained. The required power, as explained in backward approach, is then fed back into the model to obtain the required characteristics of the system.

From the simulations, we can conclude that for the modified Indian Driving Cycle and auto-rickshaw requires about 4 kW of power for 80% of the time. Only during small portions of the power requirement rises to 8 kW. The simulations also show that for a typical driving of auto-rickshaw (Driver 1 on day 11) the power requirements are much smaller. These observations suggest that a hybrid configuration can significantly increase fuel efficiency. Additionally, if the arrangement is such that most of the time the vehicle is being driven by the electric motor, the pollution will also be significantly reduced. In the next section, we present proposed speed addition concept. We also present the equations for torque addition. In the next chapter, we present simulation results and comparison of the two hybrid configurations.

2.6 Principle of speed & torque addition

A parallel hybrid vehicle consists of two or more power sources connected to the output. In a general parallel hybrid system, when the losses are ignored the mechanical speed coupler has the property [54].

$$\omega_3 = k_1\omega_1 + k_2\omega_2 \tag{2.8}$$

where, k_1 and k_2 are constants associated with the structural and geometric design of the mechanical coupler. For power conservation the torques are linked together by

$$T_3 = \frac{T_1}{k_1} = \frac{T_2}{k_2} \tag{2.9}$$

We denote the output of the IC engine by (T_1, ω_1), the output of a motor by (T_2, ω_2) and the resulting output of the hybrid configuration by (T_3, ω_3). For speed addition, with k_1 and k_2 as unity[1], T_1, T_2 and T_3 are equal and the speed of the output is given as

$$\omega_3 = \omega_1 + \omega_2 \tag{2.10}$$

In the case of torque addition,

$$\omega_3 \quad = \quad k_1\omega_1 = k_2\omega_2 \tag{2.11}$$

[1]We assume that the output is after the continuous variable transmission (CVT) used in the experiments (see chapter 4).

$$T_3 = \frac{T_1}{k_1} + \frac{T_2}{k_2} \tag{2.12}$$

for $k_1 = k_2 = 1$,

$$T_3 = T_1 + T_2 \tag{2.13}$$

$$\omega_3 = \omega_1 = \omega_2 \tag{2.14}$$

and the output speed ω_3 must be same as ω_1 and ω_2.

If k_1 and k_2 are not unity, the output speed and torque can be easily found in terms of k_1 and k_2. These are given as:

$$\begin{aligned} \omega_3 &= \frac{\omega_1}{k_1} + \frac{\omega_2}{k_2} \qquad \text{for speed addition} \\ T_3 &= k_1 T_1 + k_2 T_2 \qquad \text{for torque addition} \end{aligned} \tag{2.15}$$

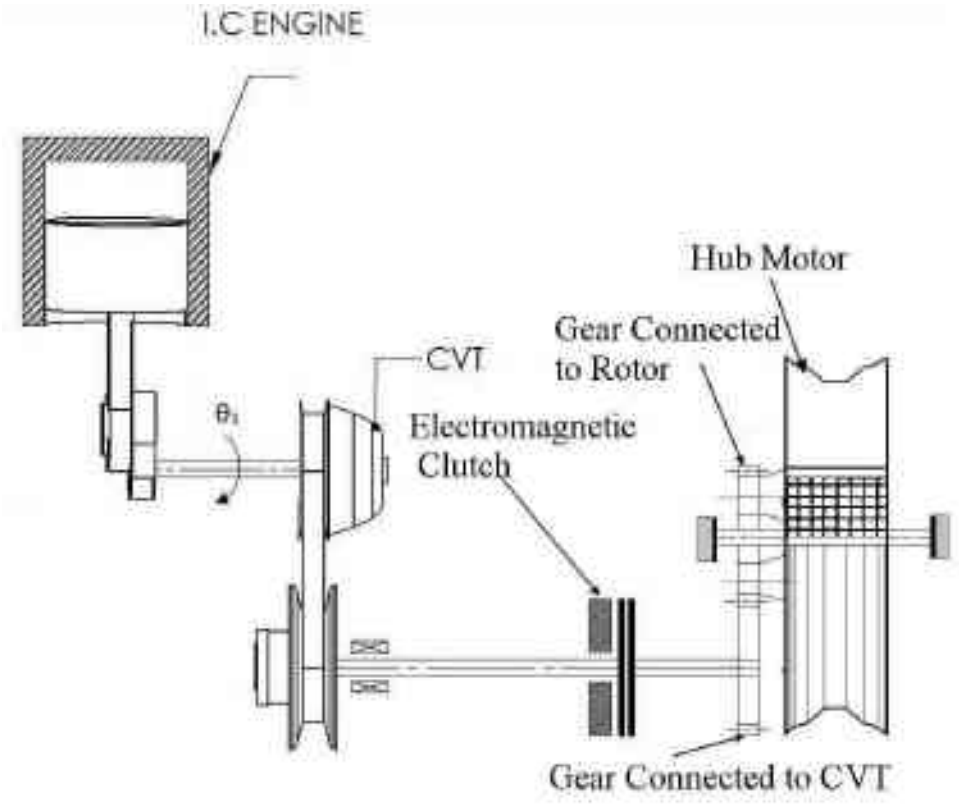

Figure 2.18: Layout of parallel hybrid vehicle with torque addition

Torque addition layout is shown in figure 2.18 It can be observed that both the power

sources i.e, IC engine and electric motor are connected through gears which results in torque addition and the speed addition configuration is described in detail in next section. The layout of speed addition is shown in figure 2.19.

2.6.1 Parallel hybrid speed addition

The schematic layout of speed addition configuration is shown in the figure 2.19. In this arrangement an internal combustion engine is connected to the wheel output through a hub motor. The addition of speed of the IC engine and the motor can take place at any speed and hence the output of IC engine is connected to a variable diameter pulley type continuous variable transmission (CVT) and the output of the CVT is connected to the stator of a conventional hub motor through an electromagnetic clutch and a spring loaded electromagnetic brake. The figure also shows a generator attached to the IC engine which can be used to charge batteries. In case of a drop in state-of-charge (SOC) of the batteries below a desired limit, the electromagnetic clutch can be disengaged and the generator can be engaged to charge the batteries. In this sense, the parallel speed addition configuration can be easily modified to a series hybrid and the IC engine can be operated at an optimum performance level to charge the battery which could then power the electric motor. In this work, we do not model and simulate the generator or the series hybrid configuration.

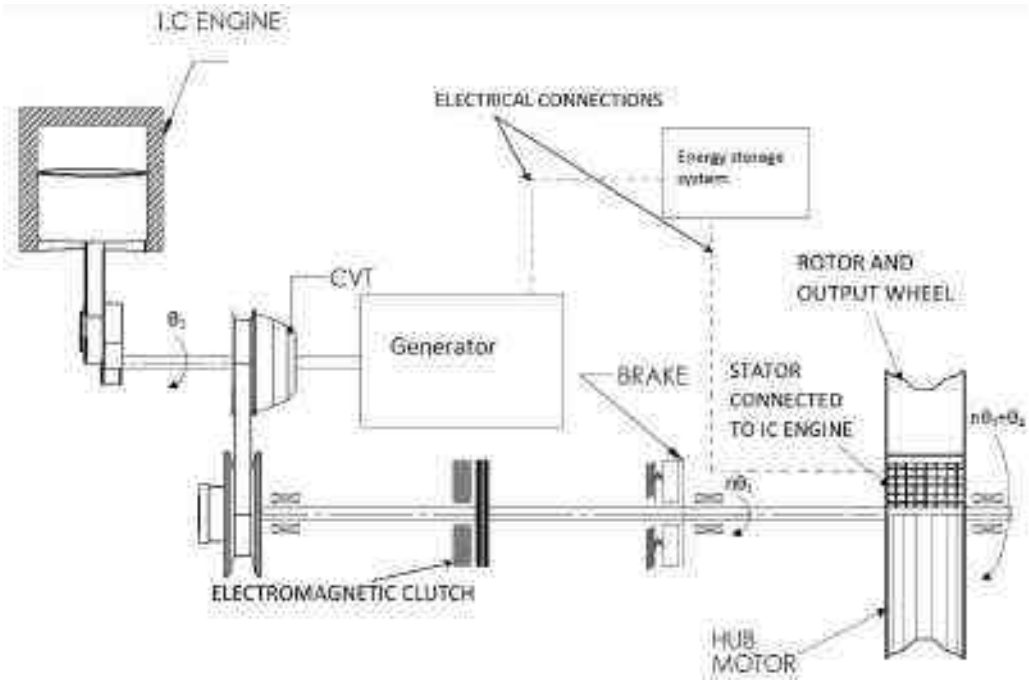

Figure 2.19: Layout of parallel hybrid vehicle with speed addition and option for series hybrid.

It maybe noted that although the kinematic arrangement of the two power sources are in series, the configuration represents a parallel hybrid as both the power sources can see the load at the wheel. The connection of the IC engine to the stator of the hub motor and the output angular velocity of the wheel being the sum of the two is widely used in serial robots [55] which was one of the source for the speed addition concept discussed in this work.

2.7 Summary

In this chapter we discuss the overall forces acting on the vehicle and effect of vehicle parameters on the torque and speed required to drive the vehicle at desired speed. We also give an overview of the actual usage of auto-rickshaw in Bangalore, India traffic to get an insight into the vehicle usage pattern. It has been observed that the actual speed that the vehicle travels is very low and the range is also limited. In the later part of this chapter we discussed various components of the vehicle and the modelling approches used in modeling them and in the final part of this chapter we introduced the parallel speed addition configuration which forms the main basis of this thesis. This configuration is differentiated from commonly used torque addition configuration.

Chapter 3

Control of a Hybrid Vehicle

3.1 Introduction

In this chapter we discuss various control strategies used in hybrid electric vehicles and the limitations and advantages of the control strategies. The discussion is in the context of the two hybrid configurations, namely speed and torque addition, presented in Chapter 2. The main function of a control system in an IC engine is either to minimize the exhaust emissions or increase the fuel economy of the vehicle. Typically, these are mutually conflicting as the exhaust emissions CO and NOx are reduced at lower temperatures whereas the fuel economy increases for higher compression ratio which results in increase in operating temperature of the engine. In a hybrid electric vehicle the control system is also used to monitor the state of charge (SOC) of the battery and the electric motor health. The control system is also used to distribute of power in case of parallel or power-split and finally control the operation of the IC engine. In this work the focus is on minimization of fuel consumption and vehicle emissions are not considered.

In this Chapter we present two control strategies for minimizing fuel consumption in a hybrid electric vehicle. The first is heuristic and the second uses dynamic programming to arrive at an optimum strategy. Both these strategies are applied on the three-wheeled auto-rickshaw for the proposed speed-addition and the typically used torque addition parallel hybrid concepts. For the heuristic approach, the results for torque addition are also compared with the results obtained from a commercial software *Autonomie* [56]. The results obtained for the Indian Driving Cycle and for a typical usage (see Chapter 2) are also presented and compared. It is shown that the speed-addition concept is better in terms of fuel economy for slow speed, start-stop urban driving.

3.2 Heuristic control strategy

Heuristics are "rules of thumb", educated guesses, intuitive judgments or simply common sense and are often the best possible or 'optimal' solutions. Many existing energy-management strategies employ heuristic control techniques. Heuristic rules are often used based on thresholds of the feedback quantities. The best example for application of heuristic control in hybrid vehicle is Toyota's Hybrid Synergy Drive [57]. The data used for modeling is described in Table 3.1.

Table 3.1: Parameters used for modeling

Parameter	Value
Weight	350Kg
Max. power	6KW@5000rpm
Frontal Area	$2.09mm^2$
Coeff. of Drag	0.5
Center of Vehicle mass	0.4m
Wheel base	1.075m
Coefficient of friction	0.015
Density of Gasoline	719.7 Kg/m^3
Fixed gear ratio	4.5

3.2.1 Heuristic control for speed and torque addition

The speed addition model uses the speed and acceleration requirement of the modified Indian Driving Cycle presented in figure 2.15. The required output power is estimated using equation (2.1). From the required power the instantaneous torque required to move the vehicle is calculated based on the speed of the vehicle. The torque required to move the vehicle is used as an input to both the IC engine and the electric motor. The motor speed is calculated and is compared with the maximum motor speed corresponding to the required torque – the torque-speed curves of the DC motor are obtained from product specifications. If the required speed is above the maximum possible speed of the motor, the engine is turned on. The input speed to the engine is the difference between the required speed and the corresponding maximum motor speed. This speed is fed to the engine model in which actual speed at which the engine is to be run is calculated based on the instantaneous continuously variable transmission (CVT) ratio. The speed and torque of the engine are recorded. The fuel consumption of the engine is calculated using the available fuel map of the engine and the recorded rpm and torque values of the engine along the drive cycle. The state of charge is computed by calculating the power

consumed by motor along the drive cycle and converting it into battery power and the resultant drop in state of charge based on the battery capacity. The total braking power that can be used to regenerate the battery is limited by the motor capacity and we assume that the rest of the braking power is supplied by mechanical braking. It is assumed that regeneration efficiency is 95% which is consistent with the data available from literature [58]. The Engine ON/OFF and torque distribution between IC engine and electric motor can be described using the flowchart shown in figure 3.1.

Similarly the engine ON/OFF and speed distribution between IC engine and electric motor can be described using the flowchart shown in figure 3.2.

3.2.2 Results of heuristic control

The torque-speed curves, drop in the state of charge (SOC) in the battery and the engine ON/OFF graphs are shown in this section and compared along with the estimated rate of fuel consumption obtained using the fuel maps of the engine. This being a hybrid the final state of charge of the batteries need to be the same as or close to the initial state of charge of the system but in this driving cycle due to braking the final SOC is same as that of initial SOC. From simulation it is observed that duration for which the fuel economy is higher in case of speed addition when compared with that of torque addition. It is due to the operating points of the engine based on the requirement.

Figure 3.3 is the total power required to drive the vehicle for parameters as shown in in table 3.1.

In figure 3.4 we can observe the engine and motor rpm the engine is higher due to the consideration of CVT gearing. This shows that even engine runs at lower throttle as the maximum rpm of engine is in the range of 7500rpm. The engine rpm plotted is corresponding to the required power that could not be met by the electric motor

In figure 3.5, we can observe the torques of both the engine and motor in speed addition configuration. The torque output of the engine before transmission is shown in this plot. The motor torque is same as the output torque as we are using a hub motor. The torque output of both engine after transmission and motor are equal and the power is added using addition of speed.

In figure 3.6 we can observe the engine ON/OFF state where '0' indicates engine is in OFF position whereas 1 indicates the engine is in ON position. The engine stays ON for 62% time of the driving cycle.

In figure 3.7 we can observe the engine and motor rpm the engine is higher due to the consideration of CVT gearing. This shows that even engine runs at higher throttle as the max-

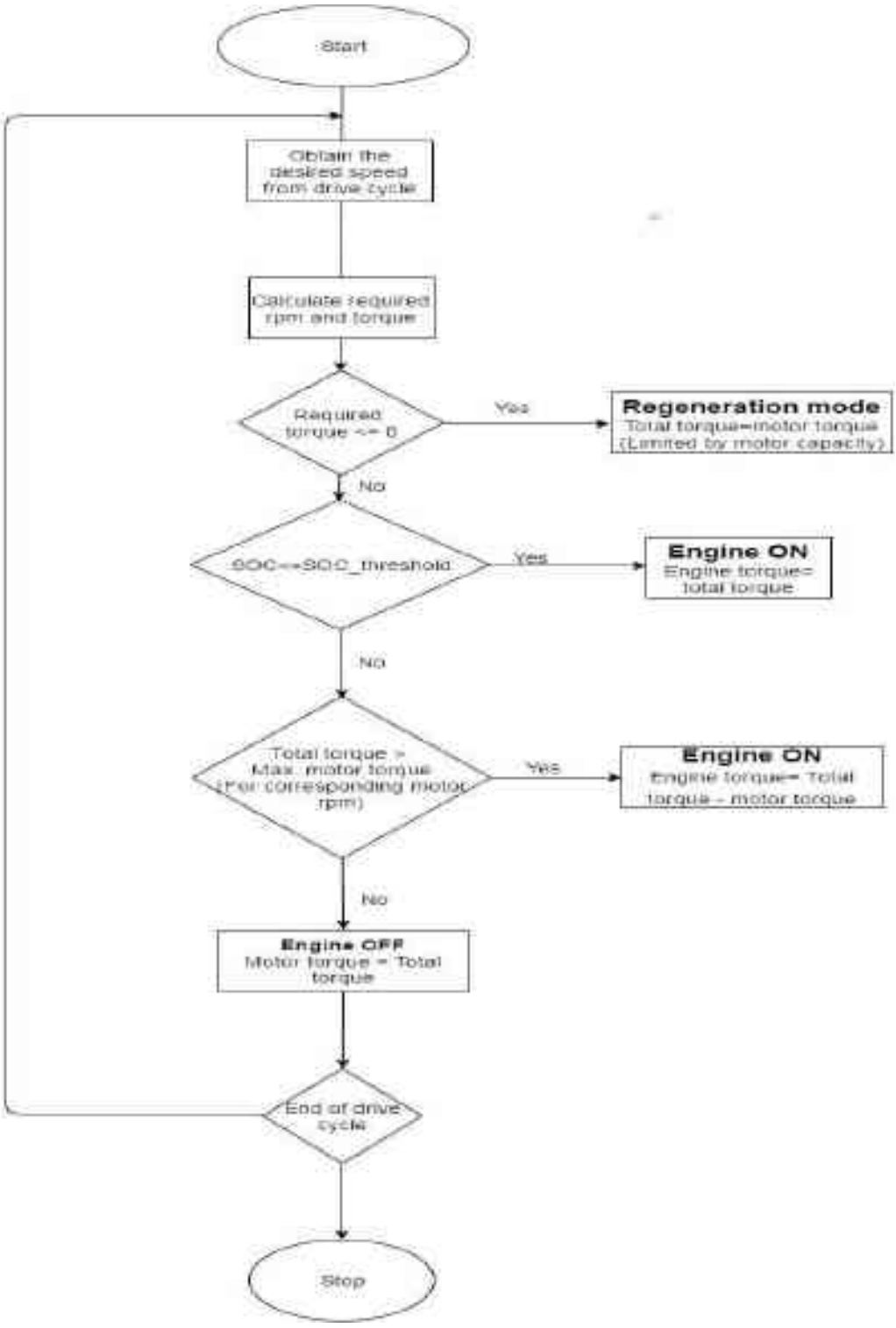

Figure 3.1: Flow chart of HEV operation in torque addition mode with heurestic control

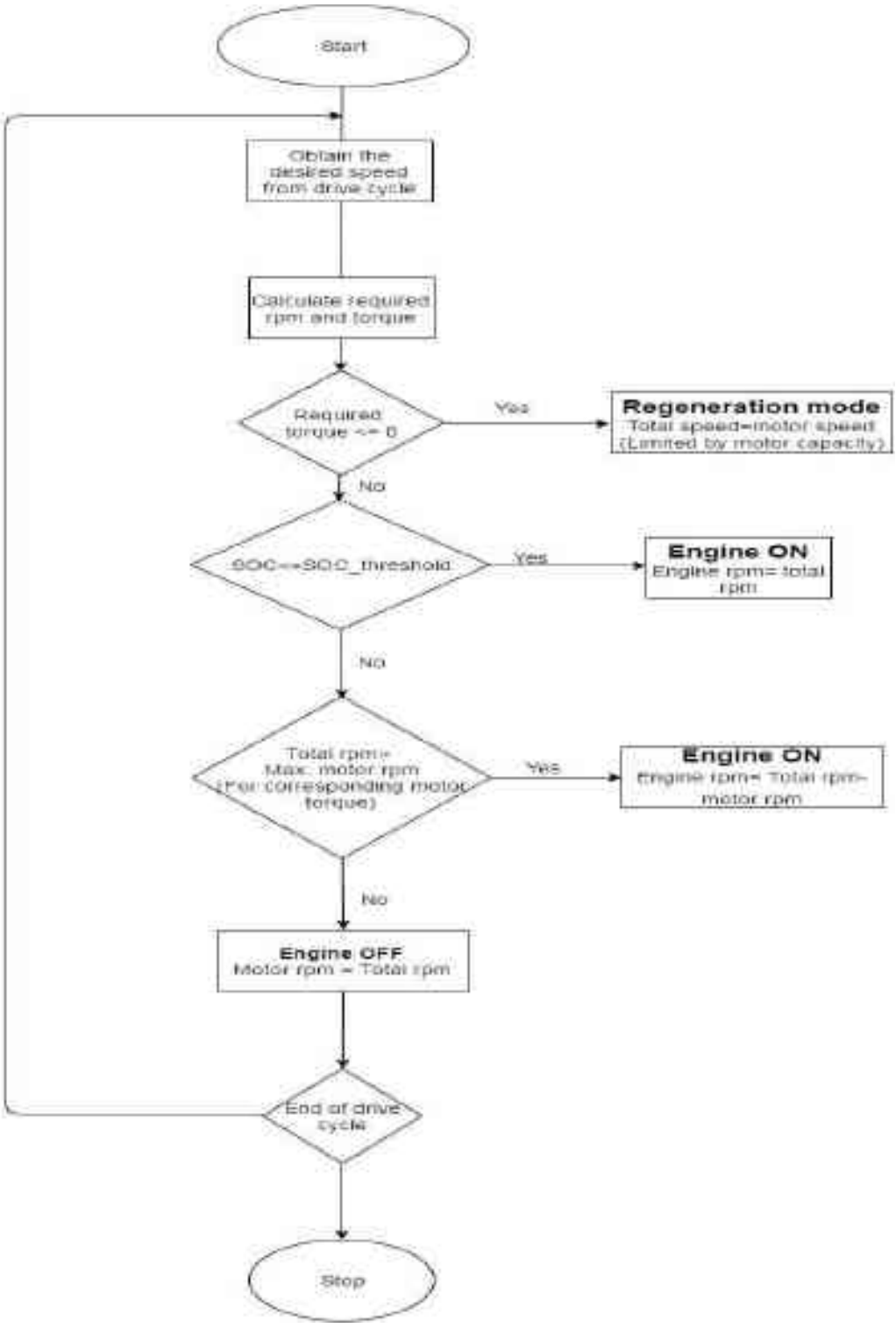

Figure 3.2: Flow chart of HEV operation in speed addition mode with heurestic control

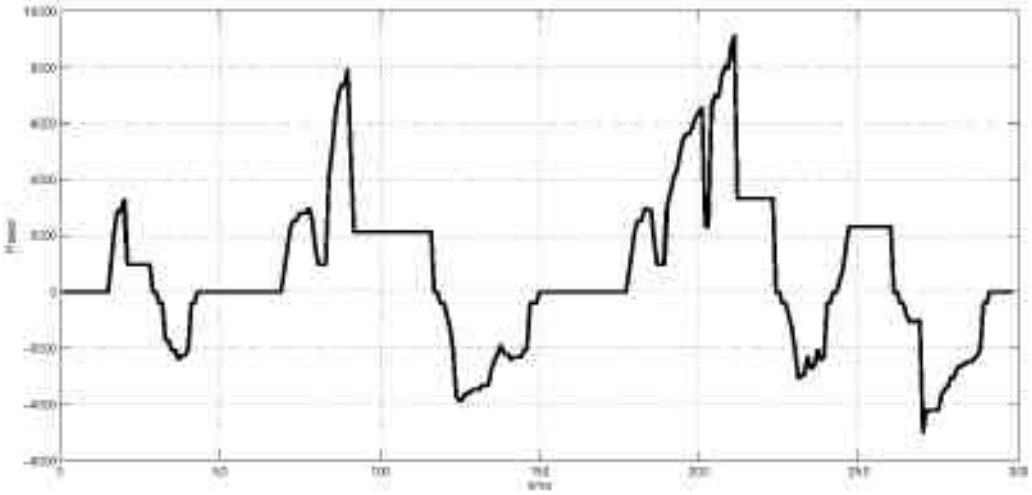

Figure 3.3: Total power required to drive the vehicle

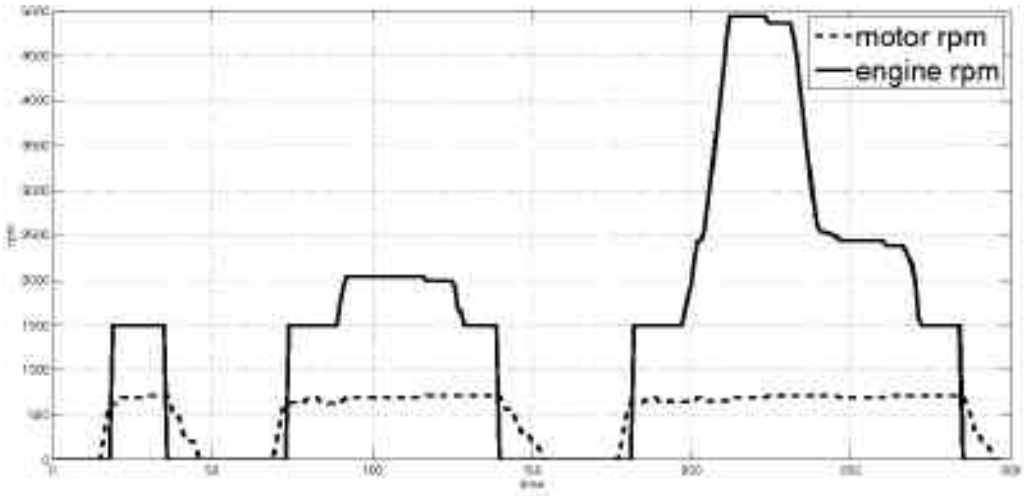

Figure 3.4: Output speed of engine (solid line) and motor (dotted line) in speed addition configuration

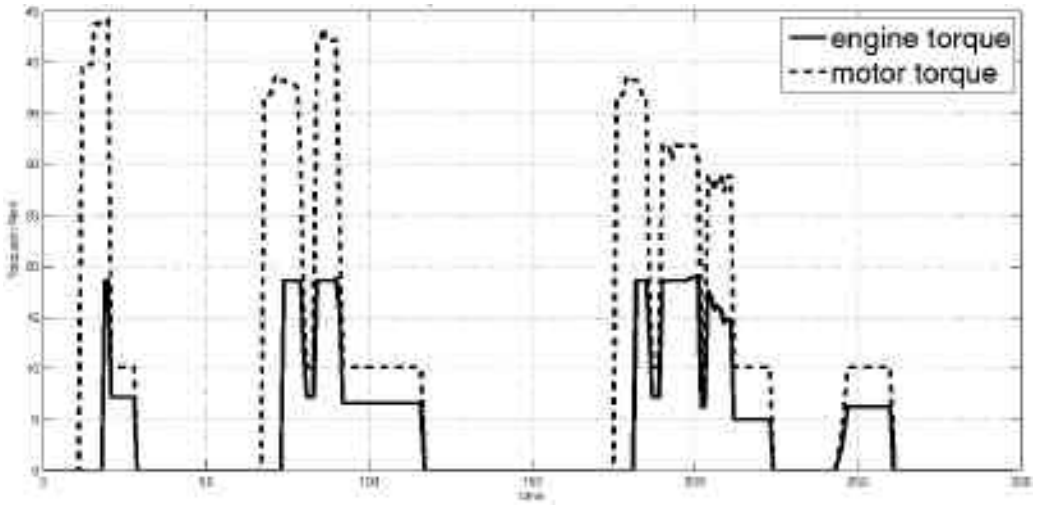

Figure 3.5: Output torque of engine (solid line) and motor (dotted line) in speed addition configuration

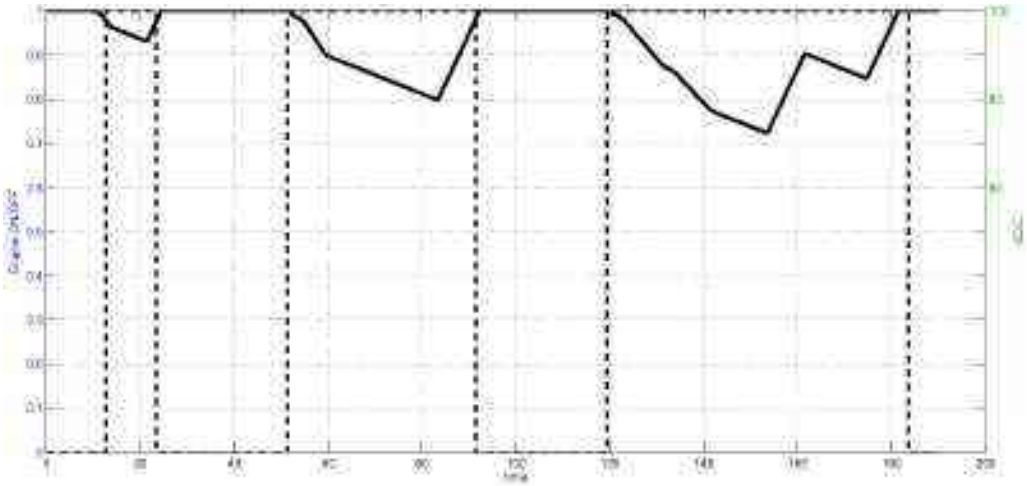

Figure 3.6: Engine ON/OFF and drop in SOC state in speed addition configuration

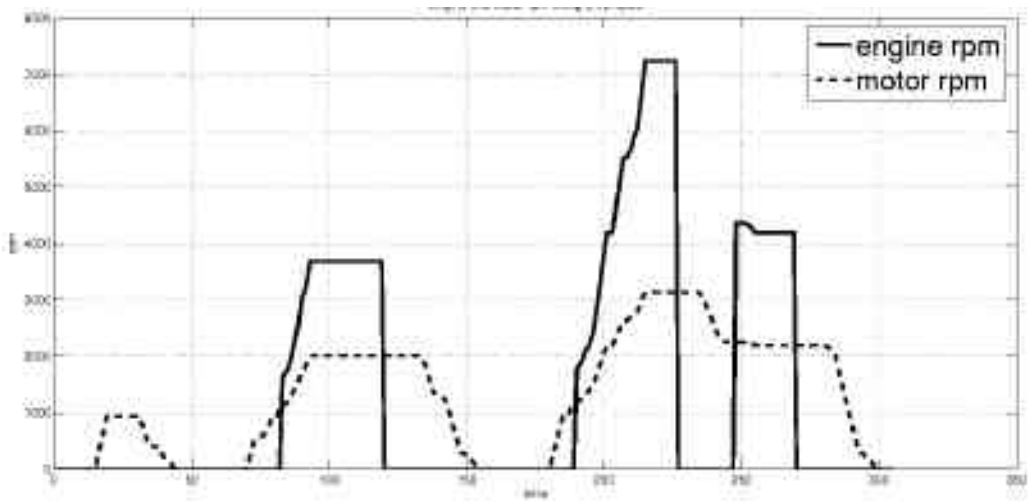

Figure 3.7: Output speed of engine (solid line) and motor (dotted line) in torque addition configuration

imum rpm of engine is in the range of 7000-7300rpm. The engine rpm plotted is corresponding to the required torque that could not be met by electric motor. The output rpm of engine after transmission and motor are same as power is added using torque addition.

In figure 3.8, we can observe the torque outputs of the engine and motor. The total required output power is obtained by adding the torques – in this case with a constant output rpm of both engine after transmission and the DC motor.

In figure 3.9 we can observe the engine ON/OFF state where o indicates engine is in OFF position whereas 1 indicates the engine is in ON position. The engine stays on for 40% time of the driving cycle. In this figure we can also observe the change in SOC where the discharging part is in acceleration and cruising part whereas the regeneration part is in the braking part of the drive cycle.

The fuel maps of engine along with the maximum efficiency line and operating points during the drive cycle in speed addition and torque addition can be observed in the figure 3.10 and figure 3.11. It can be observed that the operating points in the speed addition configuration are closer to the maximum efficiency line in number when compared to the torque addition configuration as the engine operating time is low.

From the simulation it can be observed that the speed addition setup is more efficient for urban transportation due to the lower power requirement. It has been observed that the speed addition setup gives a fuel economy of 55.72 km/l whereas the torque addition model gives a fuel economy of 32.87 km/l. The difference is mainly due to the high torque and rpm required by the engine in acceleration phase of the drive cycle. This can be clearly distinguished by

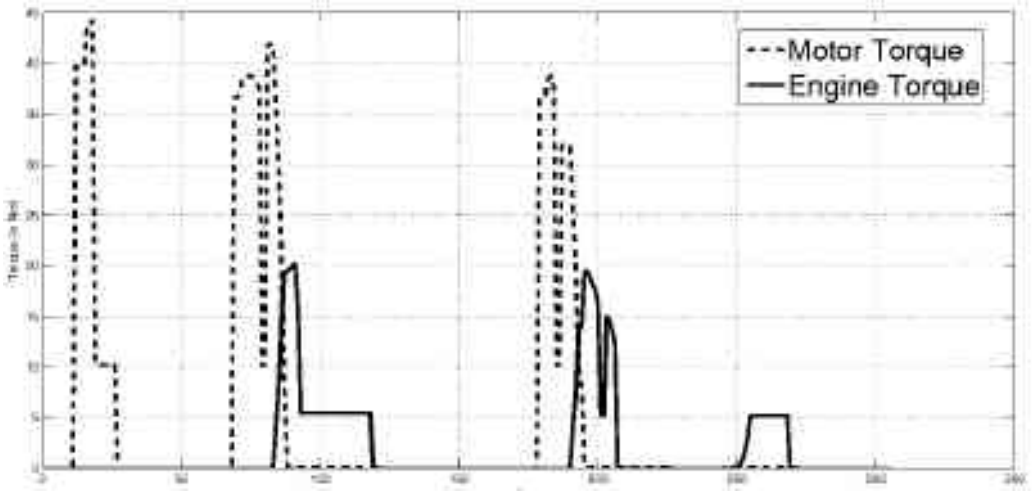

Figure 3.8: Output torque of engine (solid line) and motor (dotted line) in torque addition configuration

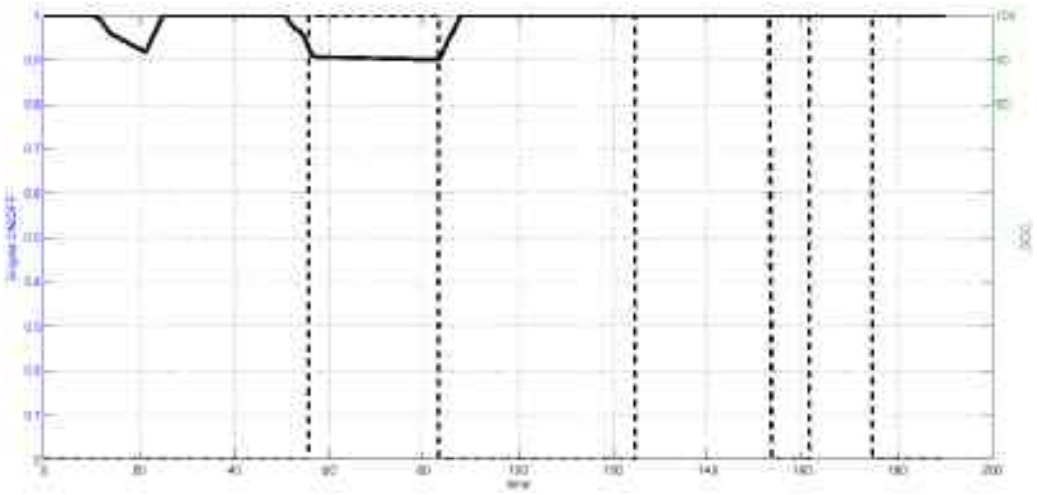

Figure 3.9: Engine ON/OFF state in torque addition configuration

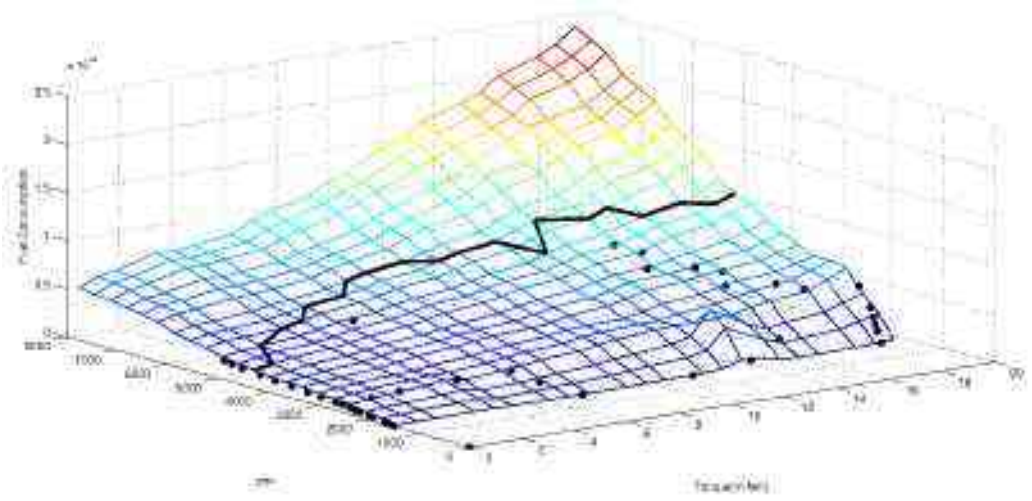

Figure 3.10: Fuel map and operating point(dots) of speed addition configuration

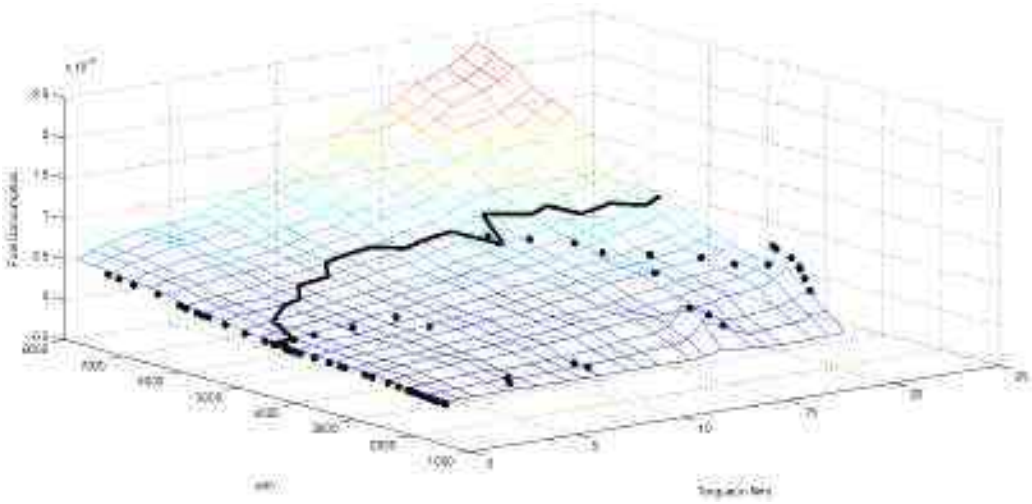

Figure 3.11: Fuel map and operating point(dots) of torque addition configuration

comparing figure 3.7and 3.4 as the rpm reaches 7200rpm in torque addition and the engine is highly inefficient at these ranges whereas in the speed addition configuration engine runs in the optimum range of 3000-5000 due to the low rpm demand as the engine speed required need not be completely met by engine alone. The addition of speed is more useful in urban setup as the stop and go traffic is more effectively handled by the electric motor.

3.2.3 Simulation results from *Autonomie*

The model for torque addition with a similar parameters has been created using the *Autonomie* software [59]. Since a model of the auto-rickshaw is not available in *Autonomie*, we modified an in-built engine model of Honda Insight engine and used the torque-speed data and fuel map supplied by General Motors for a 185 cc engine[1]. Since the engine data of the 185 cc engine is used in the *Autonmie* model, it is close to the heuristic model used for the auto-rickshaw. In addition, we have scaled down the 10 kW electric motor used in the Honda Insight to the 4 kW DC motor used in the heuristic model. The electric motor used in the Honda Insight is also not a hub motor but the power is same as the hub motor used in our model. The transmission in the Honda Insight is an automatic and we have modified the model to match the maximum and minimum gear ratios in CVT used in our model. The chassis and environment model in *Autonomie* has been modified to the specifications mentioned in Table 1.1 and 1.2.

On simulating the *Autonomie* model, we obtain the total power, the engine torque and the motor torque required for the modified Indian Drive Cycle. These are shown in figures 3.12, 3.13 and 3.14. It can be observed that the fuel economy rate is similar to that of heuristic control model for torque addition in Matlab/Simulink developed in the previous section – *Autonomie* gives 38.5 km/l is while our model gives a fuel economy of 32.8 km/l. The complete result report can be seen in Appendix B.

Autonomie does not provide a model of speed addition and hence, the results obtained for speed addition, from the Matlab/Simulink model, cannot be compared. The speed addition model is very similar to the torque addition model developed in Matlab/Simulink, with same parameters and minor but appropriate change in logic. Since the results obtained for torque addition from our model match those from *Autonomie*, we can conclude that the Matlab/Simulink models for speed and torque addition are accurate. We have used the torque and speed addition Matlab model developed for the optimal control strategy discussed next.

[1]We have used the closest model available in *Autonomie*. The Honda Insight is the smallest engine model available in *Autonomie*. It may be noted that Honda Insight is a three cylinder engine of 1000 cc capacity. The auto-rickshaw uses a 175 cc single cylinder SI engine.

Figure 3.12: Total power required to drive the vehicle from *Autonomie*

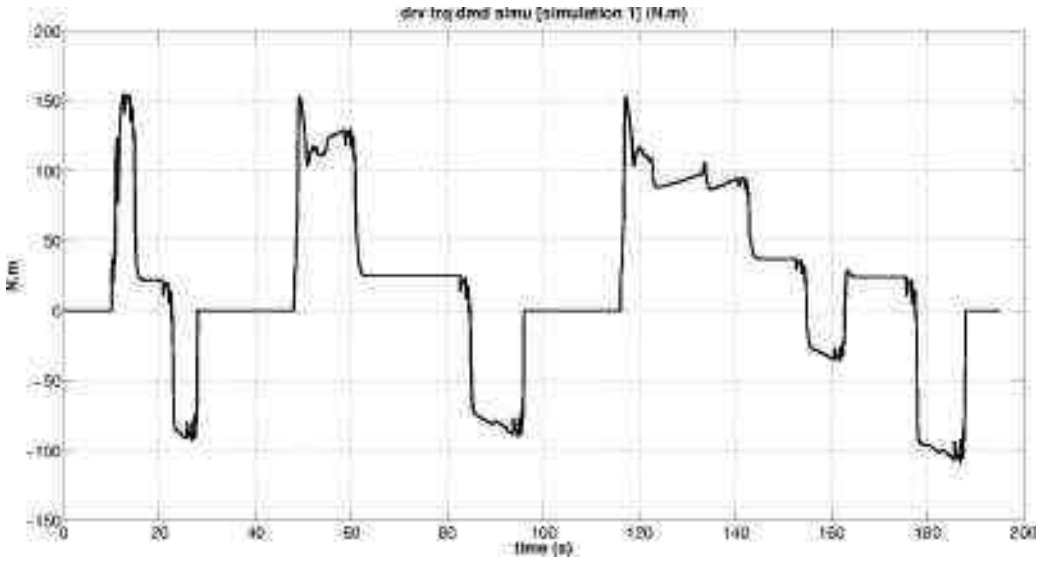

Figure 3.13: IC Engine torque from *Autonomie*

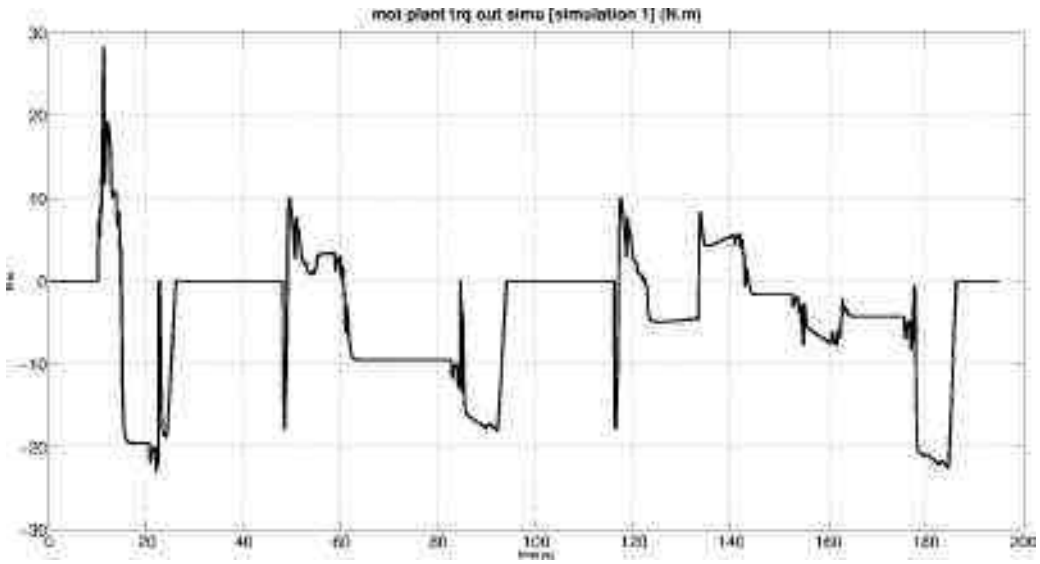

Figure 3.14: DC Motor torque from *Autonomie*

3.3 Optimal control strategy

Optimal control strategy is applicable when the drive cycle is known in its entirety. Hence cannot be applied on actual vehicle. But, we use optimal control to benchmark the performance for two different configurations. The energy management in hybrid vehicle for optimal control consists of computing a sequence of control variables such that the integral effect either minimizes or maximizes the desired quantity. The control variable considered is the hybridization or load distribution between two energy sources, i.e., IC engine and electric motor. The desired integral effect can be the minimization of fuel consumption or total pollution emission or combination of both over the entire horizon of simulation. Optimal control problems can be addressed in three different approaches

- Indirect methods
- Dynamic programming
- Direct methods

In this work we minimize the fuel consumption of the system using dynamic programming with a sequence of control signals denoting the load distribution between two different power sources.

In mathematical terms [16], consider a generic dynamic system with state equation

$$\dot{x} = f(x, u, t) \tag{3.1}$$

where $x \in \mathcal{R}^N$indicates the vector of the state variables, $u \in \mathcal{R}^m$ is the vector of the control inputs, and t denotes the time. The optimal control problem in the time interval $t \in [t_0, t_f]$ corresponds to the choice of control $u(t) : [t_0, t_f] \mapsto \mathcal{R}^m$ that leads to the minimization of the cost function (or performance index)

$$J = \phi(x(t_f), t_f) + \int_{t_0}^{t_f} L(x(t), u(t), t)dt \tag{3.2}$$

under the boundary conditions

$$\psi(t_f, s(t_f)) = 0 \tag{3.3}$$

and the local conditions

$$\begin{cases} G(x(t), t) \leq 0 \\ u(t) \in \mathcal{U}(t) \end{cases} \qquad \forall t \in [t_0, t_f] \tag{3.4}$$

where $\mathcal{U}(t)$ indicates the set of admissible control values at time t, $Lx(t), u(t), t) \in \mathcal{R}$ is the instantaneous cost function, and $\phi(x(t_f), t_f) \in \mathcal{R}$ represents the terminal cost (function of the system state at the final time).

In the case of a hybrid electric vehicle, if minimization of fuel consumption is the only objective of the controller, then L is the instantaneous fuel consumption, i.e., the mass flow rate of the fuel into the engine. In general, the cost function can be any scalar index. The terminal cost $\phi(x(t_f), t_f)$ can be used, for example, to account for the difference between the initial and final value of the state of charge in the battery. The optimization problem is also subject to several constraints. Some of the constraints are integral in nature such as the fact that the state of charge at the end of the trip must not be too different from the initial value and some are local such as instantaneous power limits, state of charge boundaries etc.. The local constraints 3.4 are instantaneous conditions that must be satisfied at each instant of time. The notation $G(x(t), t) \leq 0$ is generic; in most cases, it represents the inequalities $x_min(t) \leq x(t) \leq x_max(t)$.

The integral constraints can be enforced either as hard or soft constraints [60]. Hard constraints consist in the boundary conditions as given in equation (3.3) on the dynamic equations that constitute the optimization problem. Soft constraints, on the other hand, modify the cost function given in equation (3.2) with the term $\phi(x(t_f), t_f)$ in order to induce the final value of the constrained variable to be close, but not necessarily identical, to the desired target.

3.3.1 Dynamic programming

Dynamic programming [16, 61, 62] a numerical method for solving problems of large complexity with multistage decision making problems and is optimal control technique capable of providing the optimal solution such as minimization of fuel consumption in hybrid vehicles. For using dynamic programming technique, the entire driving cycle or entire usage cycle to be known in advance and therefore is only implementable in simulation environment. Dynamic programming is based on Bellmans principle of optimality, which can be stated as follows:

An optimal control policy has the property that no matter what the previous decision (i.e., controls) have been, the remaining decisions must constitute an optimal policy with regard to the state resulting from those previous decisions [63].

For solving the continuous control problem with final state constraints and soft local constraints using dynamic programming, the continuous time model, equation (3.1), must be discretized. Let the discrete-time model be given by

$$x_{k+1} = f_k(x_k, u_k), \quad k = 0, 1, ..., N-1 \tag{3.5}$$

with control signal $u_k \in \mathcal{U}_k$. The control policy is given as

$$\pi = u_0, u_1, ..., u_N - 1 \tag{3.6}$$

Further the discretized form of the cost function given in equation (3.2), using π with the initial state $x(0) = x_0$, is written as

$$J_\pi(x_0) = g_N(x_N) + \phi_N(x_N) + \sum_{k=0}^{N-1} h_k(x_k, u_k) + \phi_k(x_k) \tag{3.7}$$

where the first term g_N corresponds to the final cost and second term ϕ_N corresponds to penalty function forcing a partially constrained final state. The term h_k is the instantaneous cost function and ϕ_k is the penalty function for enforcing state constraint [64]. The optimal cost function is the one that minimizes the total cost

$$J^*(x_0) = min J_\pi(x_0) \tag{3.8}$$

where π is the set of all admissible policies.

Based on the principle of optimality, dynamic programming is the algorithm which evaluates the optimal cost to-go function $\mathcal{J}_k$ at every node in the discretized state-time space by proceeding

backward in time [65]. The cost for each intermediate step, for$k = N - 1$to0. is calculated as

$$\mathcal{J}_k(x^i) = \min_{u_k \in \mathcal{U}} h_k(x^i, u_k) + \phi_k(x^i) + \mathcal{J}_{k+1}(f_k(x^i, u_k)) \tag{3.9}$$

and the cost of the end step is computed as

$$\mathcal{J}_N(x^i) = g_N(x^i) + \phi_N(x^i) \tag{3.10}$$

The optimal control is given by equation (3.9) for each x^i at time index k of the discretized state-time space. The term $\mathcal{J}_{k+1}(x)$ is evaluated only on discretized points in the state space. The term $\mathcal{J}_{k+1}(f_k(x^i, u_k))$ must be evaluated appropriately considering the output of the model function $f_k(x^i, u_k)$ which can be between the nodes of the state grid. The cost to-go function $\mathcal{J}_{k+1}(f_k(x^i, u_k))$ is found using linear interpolation. The output of the equations (3.9) and 3.10 is an optimal control signal map. This map is used to find the optimal signal during forward simulation of the model 3.5, starting from the initial state to generate a optimal state output. In the map the control signal is only given for the discrete points in state space grid. The control signal is therefore interpolated when the actual state does not coincide with the points in state grid.

In this thesis we use a Boundary-Line Dynamic program [65] which improve the blurred gradient at the boundary line due to the interpolation of cost-to-go between a feasible and unfeasible state-grid point. The vehicle components are modeled as described in Chapter 2. The model equations can be described as

$$x_{k+1} = f(x_k, u_k, v_k, a_k) + x_k \tag{3.11}$$

where x_k is the battery SOC, u_k is the torque split factor, v_k is the vehicle speed, a_k is the vehicle acceleration.

Based on the modified Indian drive cycle, as shown in figure 2.15 and described in section 2.5, the vehicle speed v_k and acceleration a_k at instance k can be included into the model function to form a time variant model given by

$$x_{k+1} = f_k(x_k, u_k) + c_k \quad k = 0, 1, ..., N - 1 \tag{3.12}$$

and the cost function representing the fuel consumption over the drive cycle can be written as

$$J = \sum_{k=0}^{N-1} \Delta m_f(u_k, k) \tag{3.13}$$

The optimization problem for minimizing the total fuel mass consumed for the hybrid vehicle over the drive cycle can be stated as a discrete time optimal control problem

$$\min_{u_k \in \mathcal{U}_k} \quad \sum_{k=0}^{N-1} \delta m_f(u_k, k) \tag{3.14}$$

$$\text{s.t.}$$

$$x_k + 1 \quad = f_k(x_k, u_k) + x_k \tag{3.15}$$

where, δm_f is the fuels mass consumption at each time step defined as 1 second.

The main objective of this dynamic programming algorithm is to obtain the optimal load distribution between the electric motor and the IC engine (along with the CVT). The load distribution in case of torque addition is division of torque in between the IC engine and the electric motor with the output rpm of both the sources identical for proper functioning of the system. In case of speed addition the division is in terms of rotational velocity based on the speed of the vehicle at which it is traveling since torque output form both the sources is same. The parameters used in the dynamic programming based are according to our system model as given in Table 3.1

In the model we assume that the starting state of charge (SOC) is 0.7, a maximum SOC of 1 and minimum SOC of 0.3 and a final SOC greater than or equal to 0.7. The length of modified Indian driving cycle is 196s and since each time step is chosen as 1 sec, we have

$$\begin{aligned} x_0 &= 0.7 \\ x_N &\geq 0.7 \\ x_k &\in [0.3, 0.9] \\ N &= \frac{196}{N} + 1 \end{aligned} \tag{3.16}$$

Considering the above mentioned initial conditions and other constraints and the nature of system we discretize the control signal from 1 to -1 in steps of 0.1 where 1 indicates that the vehicle runs on electric motor only with the engine completely switched off and 0 it implies that the vehicle is completely run by IC engine and the electric motor is not used to run the vehicle or to recharge the battery. In-case of a control signal of -1 the engine takes care of vehicle load as well as it charges the battery using the same capacity. The modeling has been done such that the control signal can be varied according to the engine size such that it can recharge the batteries. The dynamic programming has been done using Matlab/Simulink and the dynamic program optimization function that has been used is a readily available optimization algorithm [65].

The results obtained from dynamic programming are discussed next.

3.3.2 Results of dynamic programming

The total torque required for the vehicle has been calculated using the energy balance equation (2.1) and vehicle parameters described in Tables 1.1 and 1.2. The total required torque and angular velocity of the vehicle for Modified Indian Driving Cycle as described in Section 2.5 is given in Figures 3.15 and 3.16. It can be observed that the maximum torque required is 96 Nm and the holding torque of 11.64 Nm is required due to the gradient considered even when the vehicle is at rest. The maximum amount of braking torque required is 54.5 Nm and this is generally absorbed to recharge the battery using regenerative braking. The regenerative braking is limited by motor capacity and any extra energy to be dissipated is assumed to be dispersed using mechanical brakes. The total rpm is similar to Figure 2.15 since it purely depends on the drive cycle and the linear velocity is converted into angular velocity at the wheel. It can be observed from figure 3.16 that a maximum rpm of 61.46 rad/sec when the vehicle is traveling at a speed of 50 Kmph.

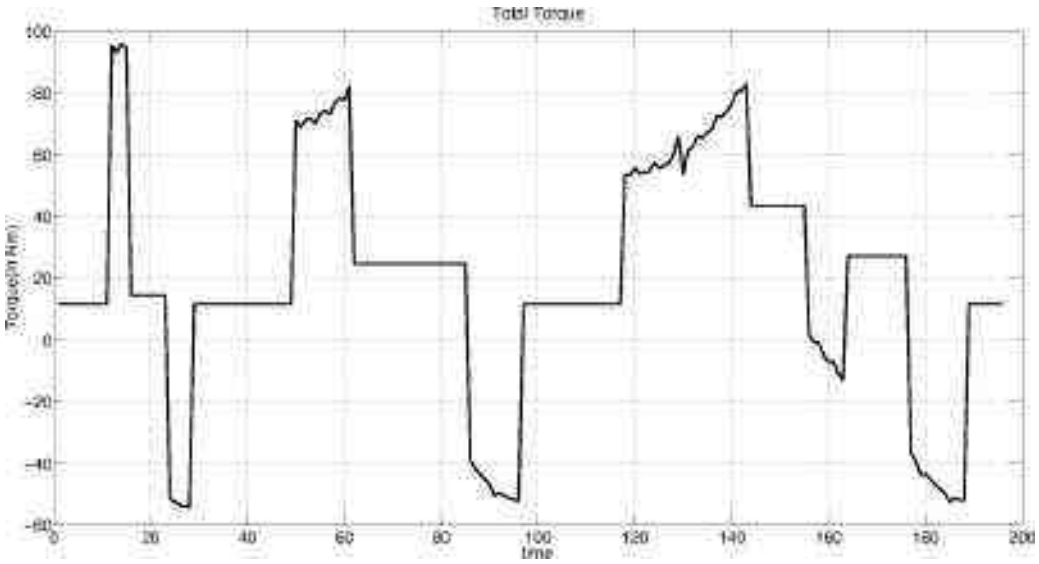

Figure 3.15: Total torque required at the wheel to drive the vehicle

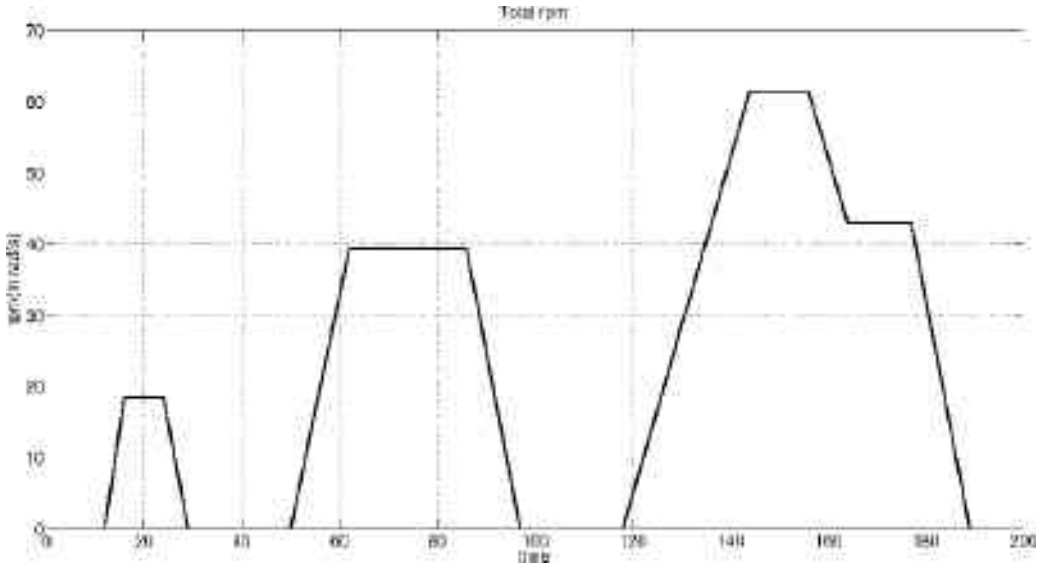

Figure 3.16: Total rpm required at the wheel to drive the vehicle

In figure 3.17 we can observe the optimal distribution of load between both the engine and electric motor. The control signal varies from a values of 1 to -1 in steps of 0.1. As mentioned 1 indicates a pure electric drive and zero indicates the vehicle is driven completely by IC engine and -1 Indicates the vehicle is driven as well as battery is replenished using the IC engine.

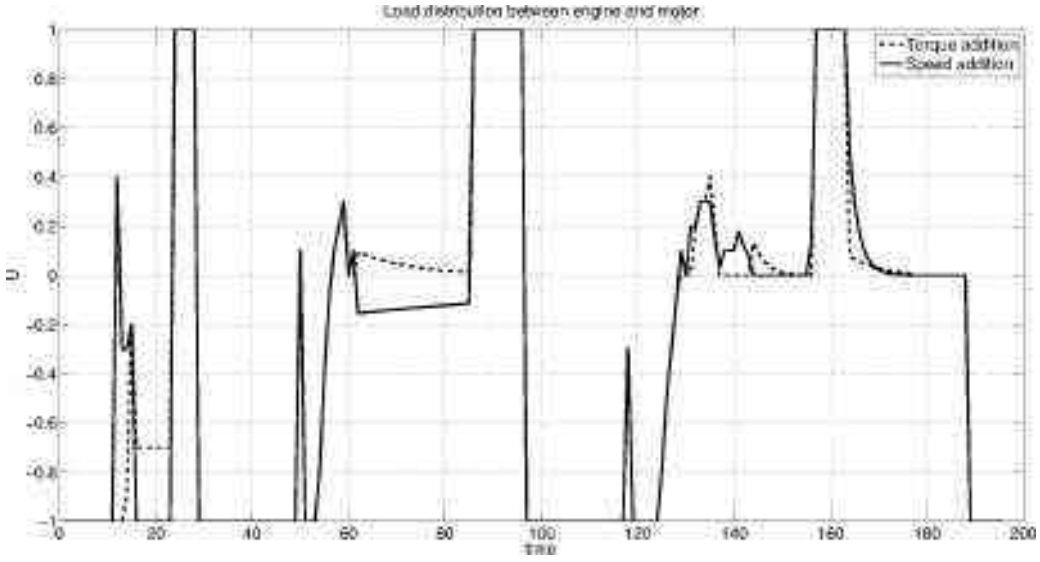

Figure 3.17: Load distribution between electric motor and IC engine for speed addition (solid line) and torque addition (dotted line)

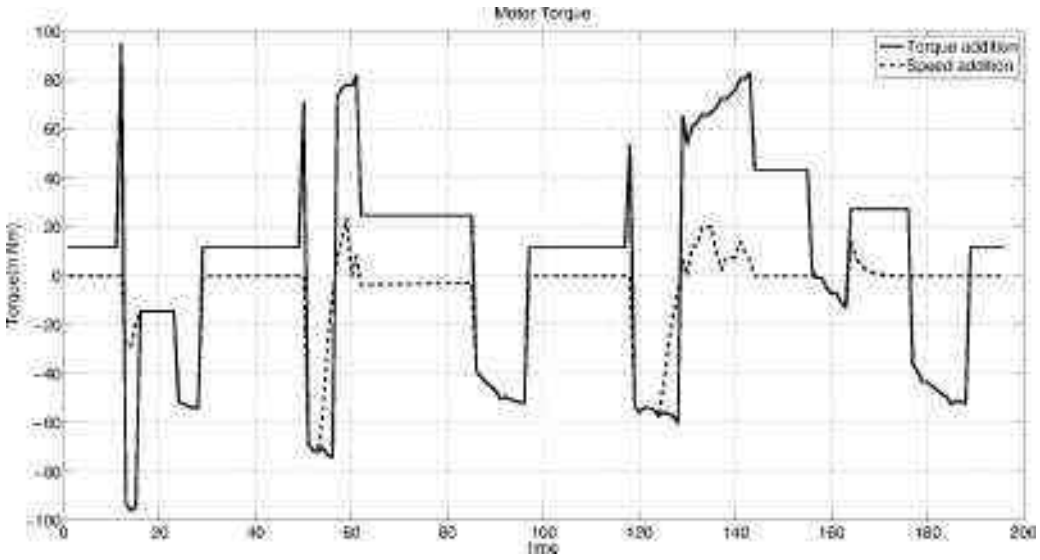

Figure 3.18: Motor torque for for speed addition(solid line) and torque addition(dotted line)

In figure 3.18 the motor torque of both the configurations are shown. The motor torque in speed addition is higher on both positive and negative torques when compared to torque addition configuration because the total torque is supplied by the electric motor as well as engine (along with CVT), thereby resulting in higher torque for speed addition configuration.

In figure 3.19 the engine torque of both the speed addition and torque addition configuration are shown. The engine torque similar to motor torque is higher in speed addition configuration but the CVT and fixed gear ratio takes care of the higher torque resulting in the torques shown in figure 3.19.

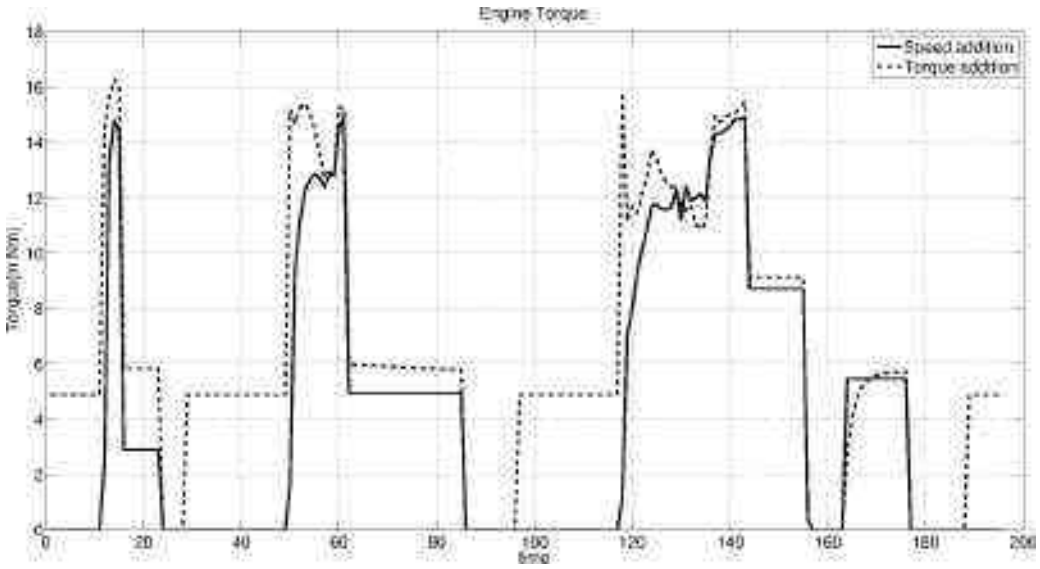

Figure 3.19: Engine torque for speed addition (solid line) and torque addition (dotted line)

In figure 3.20, the motor rpm along the drive cycle for both speed addition and torque addition configuration are shown. The motor rpm for torque addition is similar to total required rpm because of lack of any mechanical transmission of gears in between the output and electric motor and in torque addition the total rpm is equal to both the motor rpm and engine rpm after transmission.

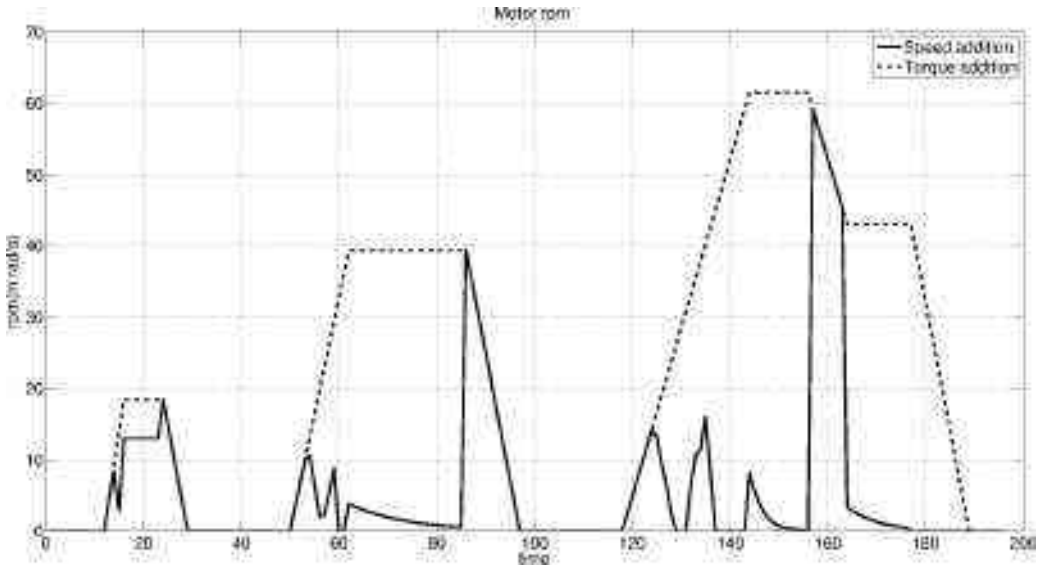

Figure 3.20: Motor rpm for speed addition (solid line) and torque addition (dotted line)

In figure 3.21, the engine rpm along the drive cycle for both the speed addition and torque

addition configuration are shown. The plot represents the actual engine rpm not the rpm share of engine and CVT combined rpm of the hybrid.

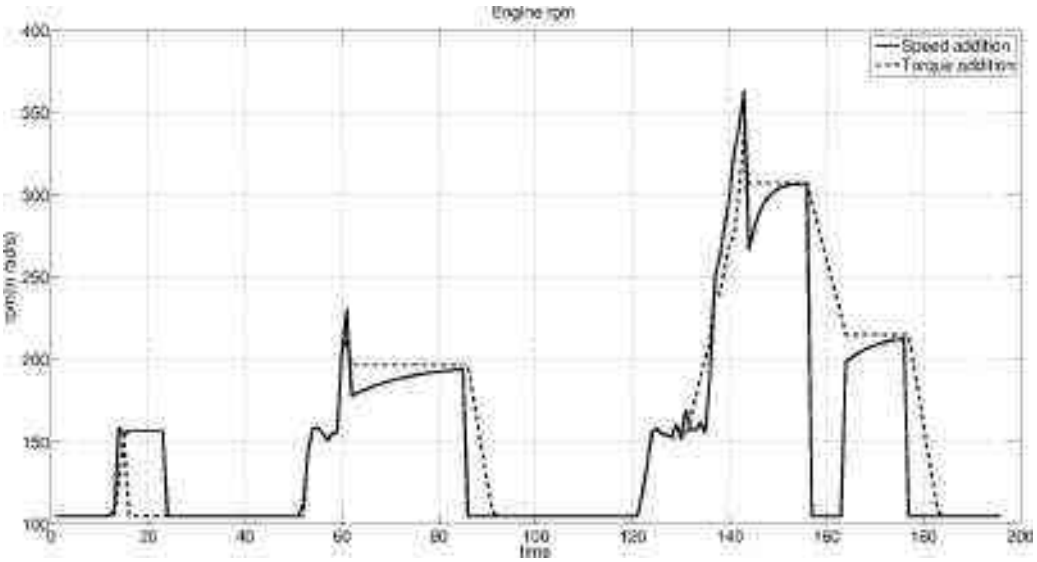

Figure 3.21: Engine rpm for speed addition (solid line) and torque addition (dotted line)

The main aim of applying dynamic programming for hybrid configuration is to benchmark the fuel consumption of both the configurations and compare them for a drive cycle. The optimal control of dynamic programming considers the whole drive cycle and the final condition is similar to initial condition resulting in no drop in SOC. It has been observed that the torque addition configuration gives a fuel economy of 91.88 km/l whereas the speed addition model gives a fuel economy 98.03 km/l. This higher efficiency is mainly due to the usage of the electric motor for higher torque requirements instead of the IC engine.

3.4 Dynamic programming applied to actual usage

The dynamic programming has been applied on actual vehicle to obtain the fuel economy and control signals of each driver for every single day. The model parameters are assumed to be same as mentioned in table 3.1. It is assumed that the vehicle is switched OFF during halting and those particular set of data points are not considered while calculating fuel economy of the vehicle. The fuel consumption of the vehicle is only dependent on the acceleration and deceleration of the vehicle. It is however not dependent on the range of vehicle as the vehicle model is considered such that the final SOC is greater than or equal to the initial SOC. The average fuel consumption of each driver is mentioned in the Table 3.2. From the Table 3.2 it can be observed that the speed addition configuration gives a better fuel economy compared

Table 3.2: Summary of data collected

Driver	Avg. distance	Fuel econ. in speed add.	Fuel econ. in torque add.
Driver 1	82.4 km	67.8 km/l	63.57 km/l
Driver 2	74.95 km	86.58 km/l	75.93 km/l
Driver 3	66.80 km	87.47 km/l	72.42km/l
Driver 4	68.25 km	77.22 km/l	66.16 km/l

to that of torque addition configuration irrespective of the driving habit or the range of the vehicle.

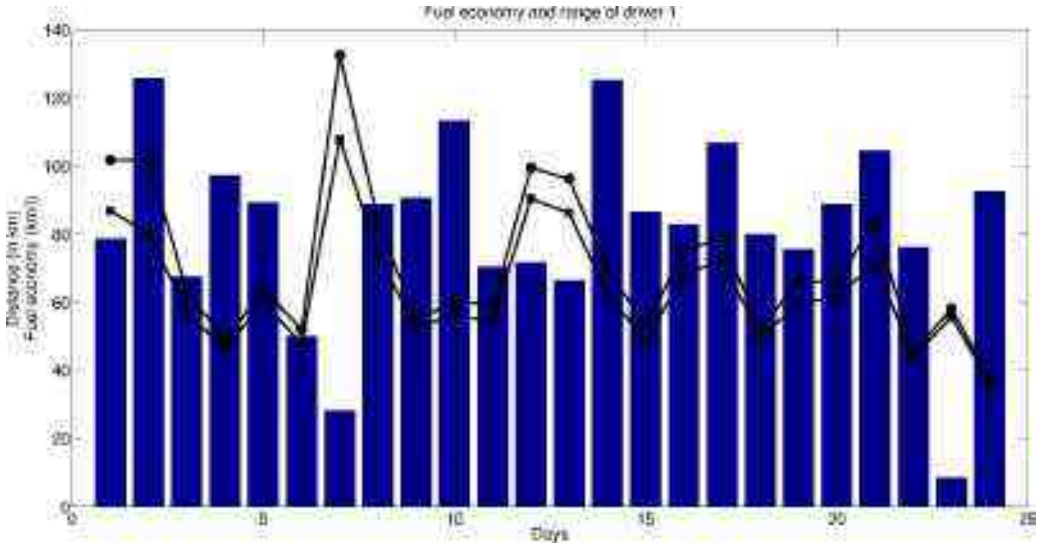

Figure 3.22: Range and fuel economy rate of speed addition and torque addition of driver 1.

It can be clearly observed from figures 3.22, 3.23, 3.24 and 3.25 that the speed addition configuration gives a better fuel economy number when compared to that of torque addition configurations. For all the four drivers the fuel economy difference for both the configurations vary from 1.3 km/l to as high as 49.14 km/l. The fuel economy is independent of the range of the vehicle and is dependent on the driving habits of each driver, primarily on fluctuation of speed or the acceleration of the vehicle. This can be clearly seen in the case of Driver 3 for days 3 and 15. The fuel economy obtained is 15.74 km/l and 53.41 km/l, respectively in case of torque addition and 20.31 km/l and 73.95 km/l, respectively in case of speed addition configuration. We have intentionally used the particular days with small ranges of 12.73 km and 15.65 km, respectively since we can then distinguish the difference in speeds more clearly – in other days with larger ranges the differences in accelerations during the full day is not as pronounced. The fluctuations in speed are shown in figures 3.26 and 3.28 for Driver 3 on day 3 and 15, respectively. The plot of acceleration for the same driver and for the same days are

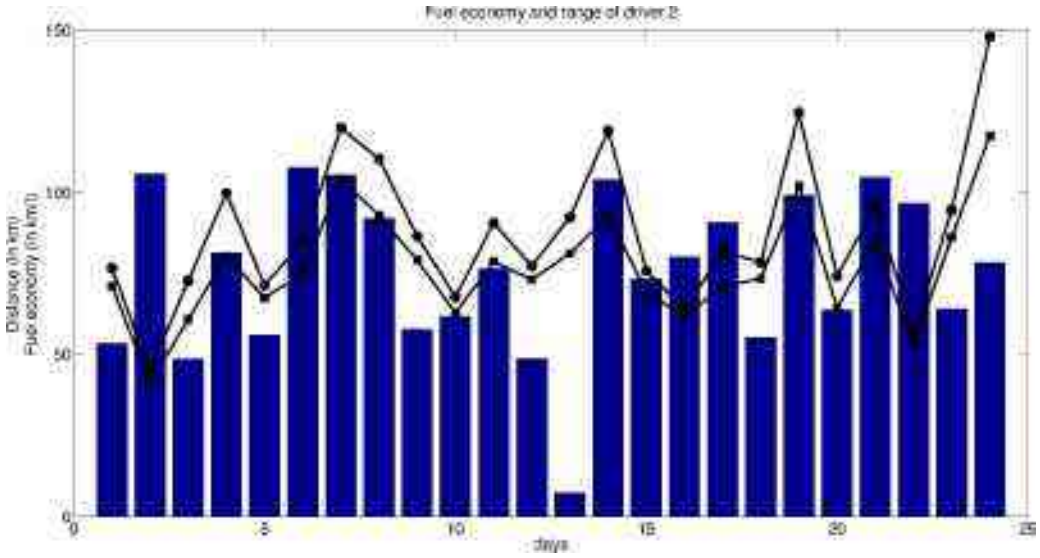

Figure 3.23: Range and fuel economy rate of speed addition and torque addition of driver 2.

shown in figures3.27 and 3.27. It can be seen that the fluctuations in speed and acceleration is more on day 3 when compared to day 15 giving rise to a lower fuel economy on day 3.

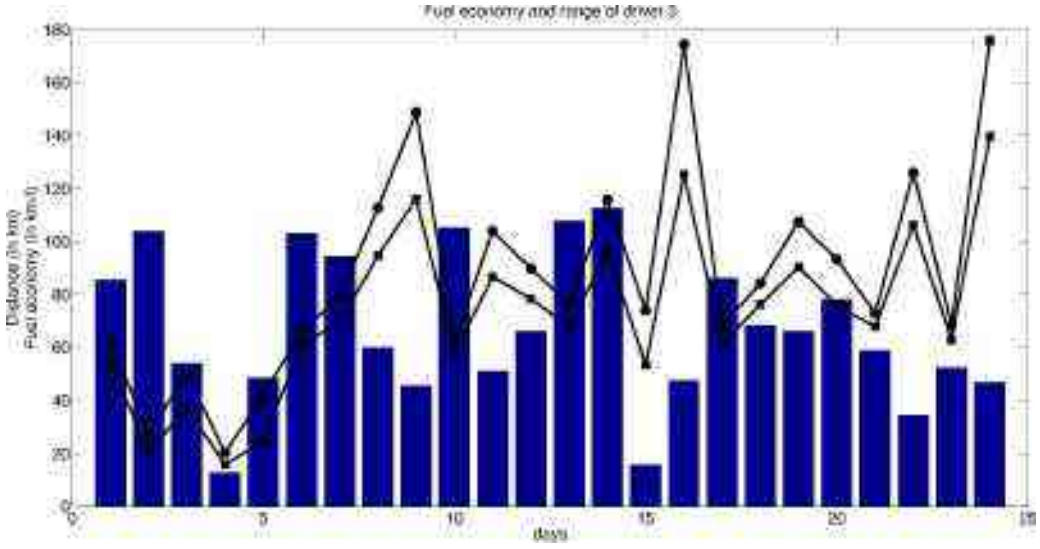

Figure 3.24: Range and fuel economy rate of speed addition and torque addition of driver 3.

3.5 Summary

In this chapter we presented control strategies for speed and torque addition configuration which can be applied to an actual vehicle and the chosen driving cycle. The torque addition model is validated using the results obtained from the commercial software *Autonomie*. The fuel

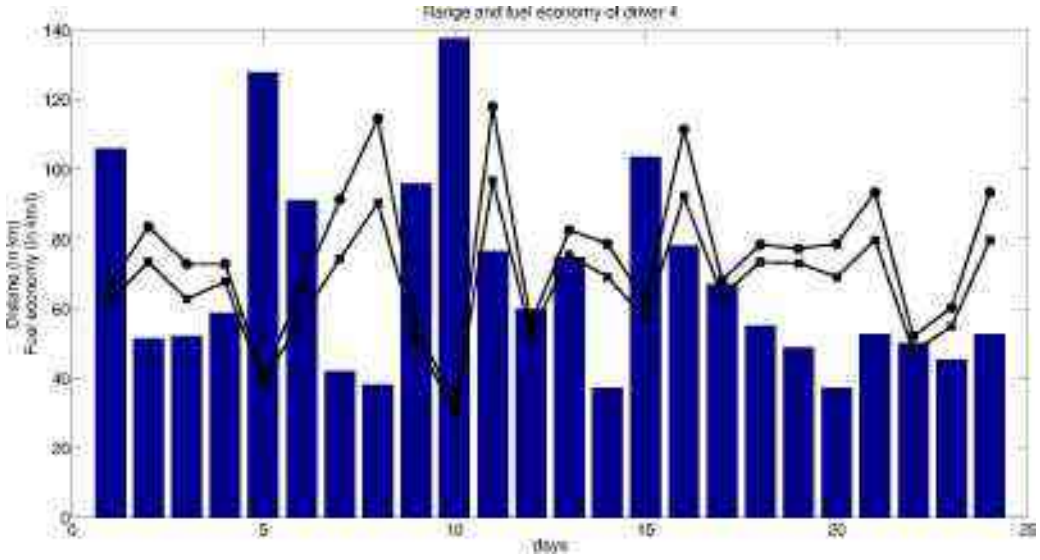

Figure 3.25: Range and fuel economy rate of speed addition and torque addition of driver 4.

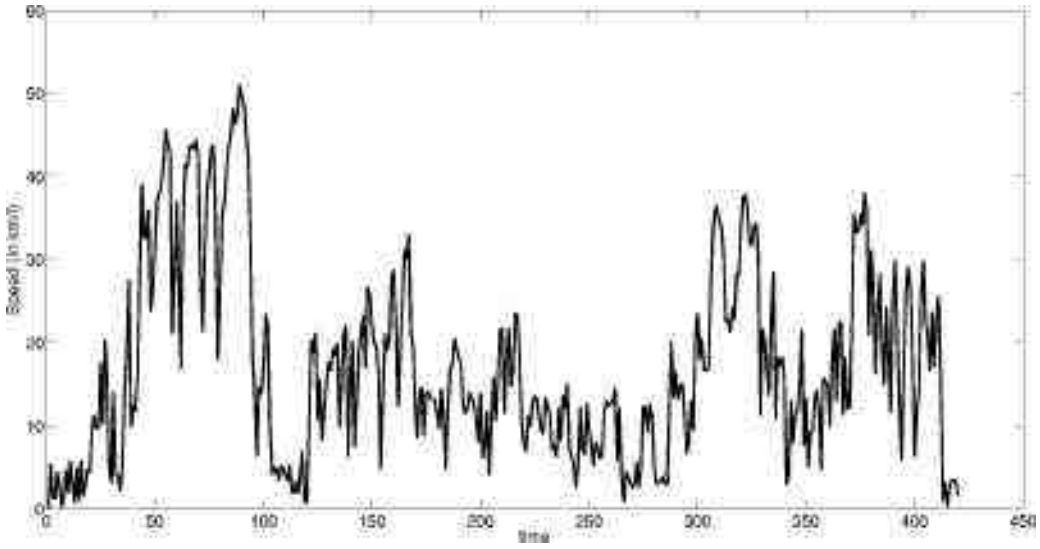

Figure 3.26: Variation of speed for driver 3 on day 3

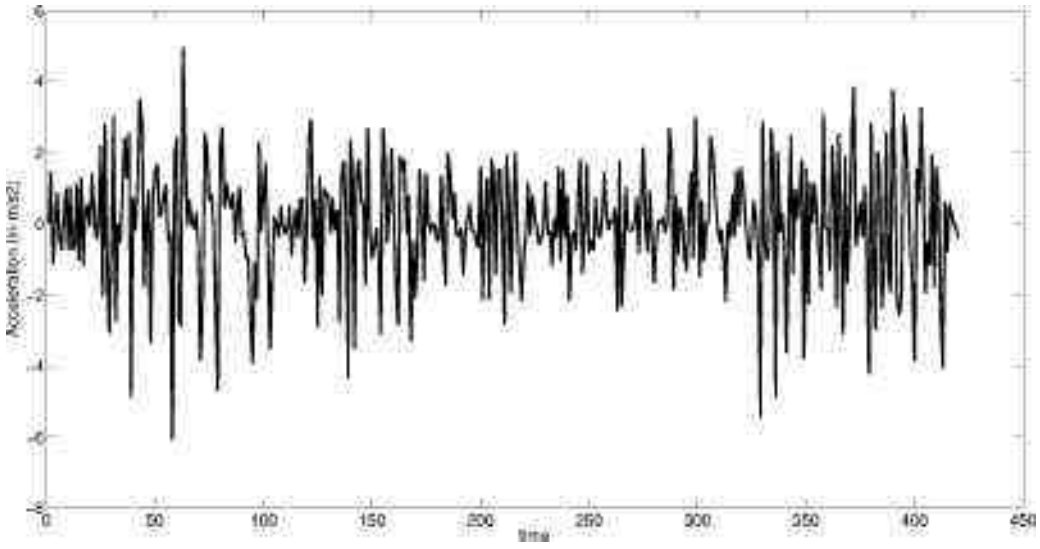

Figure 3.27: Variation of acceleration for driver 3 on day 3

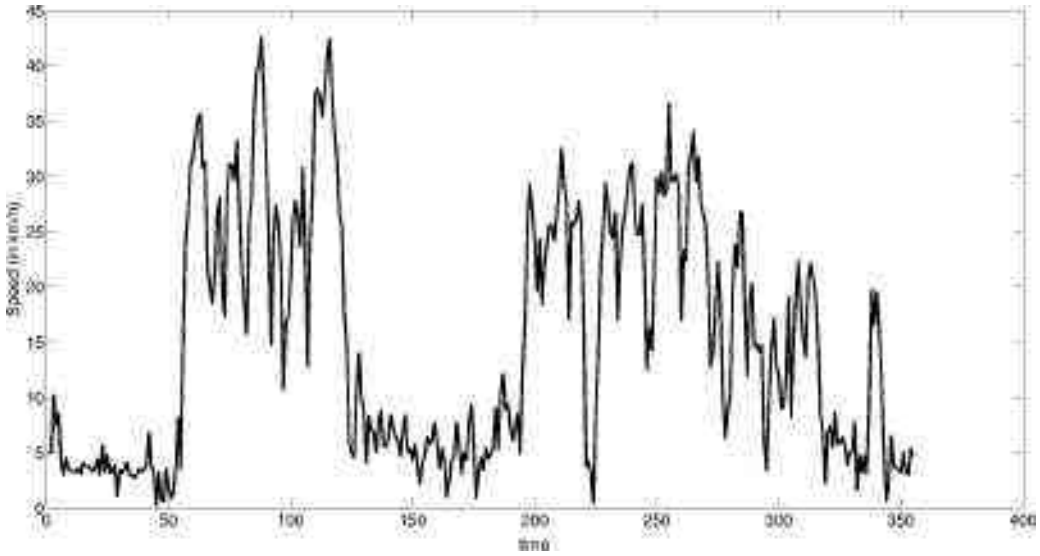

Figure 3.28: Variation of speed for driver 3 on day 15

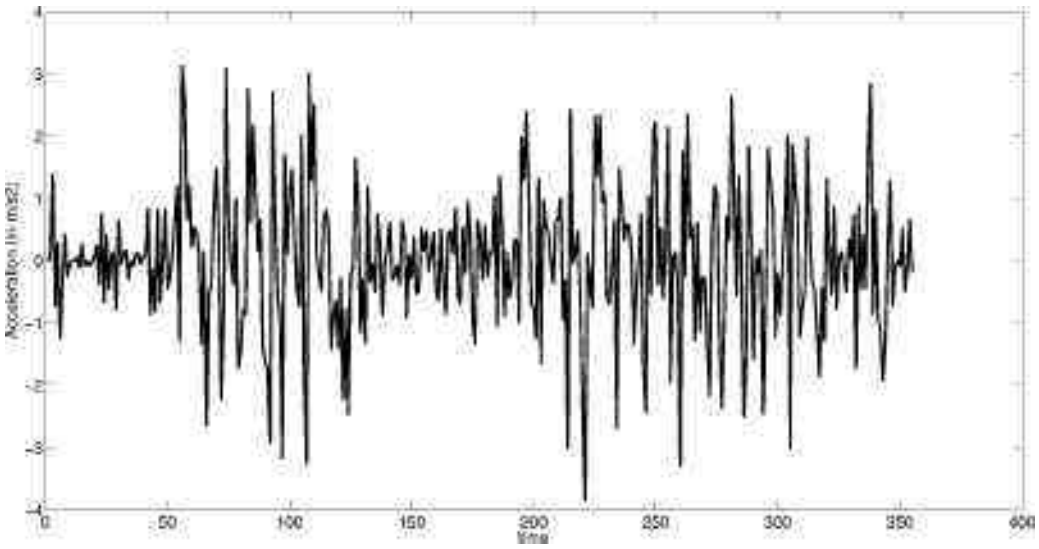

Figure 3.29: Variation of acceleration for driver 3 on day 15

economy of the speed addition and torque addition configuration are obtained using a heuristic control and the obtained fuel economy results are explained using the operating points on the fuel map. The chapter also presented a dynamic programming based optimal control strategy and results obtained from using the dynamic programming approach. The fuel economy results obtained from the heuristic and optimal control show that the speed addition configuration is better than the torque addition configuration for the chosen modified Indian Driving Cycle. The speed addition configuration also gives better fuel economy when applied on actual usage data obtained using GPS and presented in Chapter 2. In the next chapter we present experimental results obtained from a test-bed where the two parallel hybrid configurations were implemented.

Chapter 4

Experiments on a test-bed

4.1 Introduction

In this chapter we discuss the experimental setup created for validation the concept of speed addition. We also describe another similar setup for obtaining experimental results for the torque addition configuration and compare the results obtained from the two configurations. All the components used in the test-bed and the experimental approach is in descried in detail. It may be noted that the test-bed is stationary and is not for obtaining or verifying fuel efficiency results presented in the previous chapter.

4.2 Experimental test-bed

The kinematic layout of the experimental setup for speed addition was shown in Chapter 2 and is reproduced here in figure 4.1 for ready reference. It can be observed that the layout of the powertrain components is in serial but the power flow is in parallel as the power is added to the powertrain from IC engine and electric motor. The specifications of the actual components used in the experimental setup are close to those used in modeling in previous Chapters. In the experimental setup a single hub motor of 2 kW is used instead of two hub motors in the rear wheels of auto-rickshaw as modeled in previous Chapters.

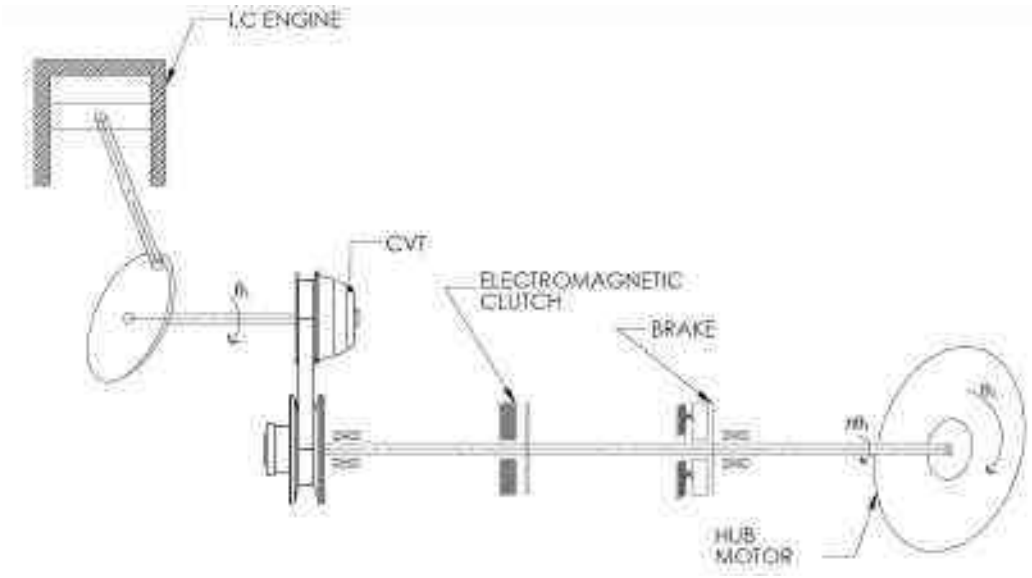

Figure 4.1: Kinematic layout for hybrid propulsion with speed addition

The experimental setup for speed addition configuration consists of a 175 cc single cylinder gasoline engine coupled with a CVT. The output of CVT is connected to one end of the electromagnetic clutch. The other end of the electromagnetic clutch is connected to the stator of 2kW brushless DC hub motor [66] through a spring loaded electromagnetic brake. The hub motor is connected to the controller using the slip ring for a the main power supply and another slip ring is used to connect the Hall sensors used to sense the rotation of the hub motor. The rotor of the hub motor is connected to an eddy current dynamometer to provide variable load. Figure 4.2 shows a photograph of the the experimental setup for speed addition. As mentioned in the kinematic diagram, the components are located in series but the actual power flow takes place in parallel. The IC engine power flows through the CVT, clutch and the brake to be added to the electric power from batteries flowing through controller, slip rings and the hub motor.

Figure 4.2: Actual experimental setup for hybrid propulsion with speed addition

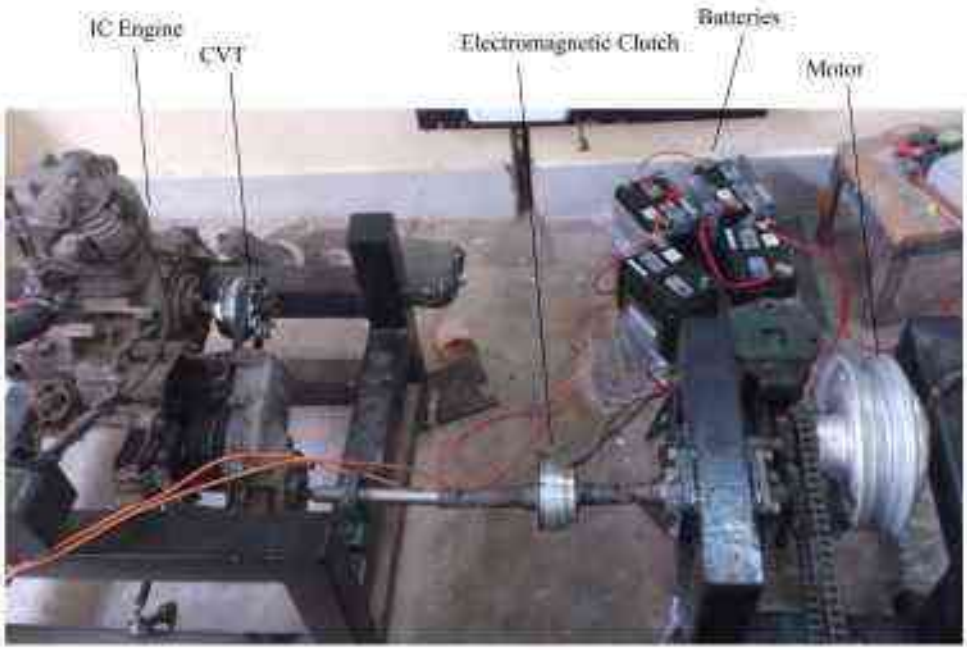

Figure 4.3: Actual experimental setup for hybrid propulsion with torque addition

In case of torque addition configuration the same 175cc single cylinder gasoline engine is

connected to rotor of 2kW brushless DC hub motor through a electromagnetic clutch using a 1:1 spur gear arrangement. The stator of the hub motor is fixed to the test-bed frame. This setup does not include any slip rings since there is no movement of stator of DC hub motor. Figure 4.3 shows the experimental setup for torque addition.

4.3 Experimental components

In this section we describe the components used in experimental setup and the specifications of each components are shown. The specifications of the components are similar to the data used in simulation and control of the hybrid engine as discussed in Chapter 2 and 3.

4.3.1 IC engine

The IC engine chosen was a 175 cc, single cylinder two-stroke used in Bajaj auto-rickshaws [33]. The IC engine is capable of developing about 7 bhp (5.15 kW) at 5000 rpm. The engine was purchased and refurbished for the experimental test-bed.

4.3.2 Permanent magnet DC hub motor

The main specifications of the chosen motor are

Table 4.1: DC motor specifications

Model	Hub Motor 48V 2KW(disc-brake)
Voltage	48V
Power rate	2000W
Weight	14kgs

The chosen hub motor is shown in figure 4.4.

Figure 4.4: DC hub motor

4.3.3 Electromagnetic clutch

An electro-magnetic clutch is used to connect/disconnect the engine from output. The clutch is supplied by Crytron Magna Drives, Thane [67]. The main specifications of the clutch are

Table 4.2: Specifications of shaft mounted clutch

Model	Shaft Mounted Clutch 170mm design:2.1
Voltage	48V
Torque	120Nm
Max Speed	3500rpm
Input Power	50W

The model of clutch is shown in figure 4.5.

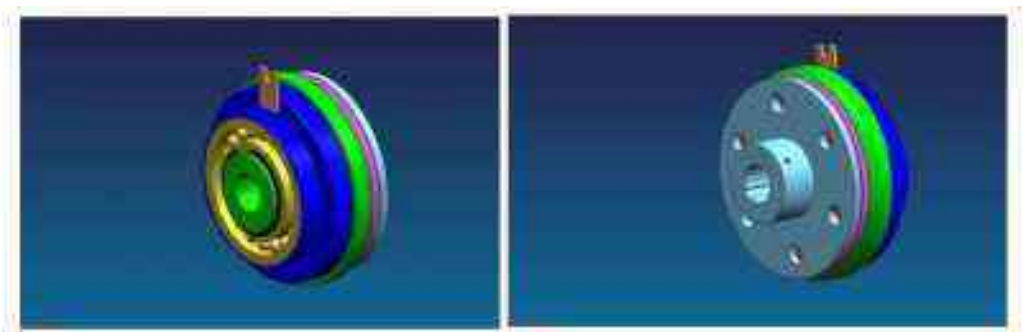

Figure 4.5: Shaft mounted clutch

4.3.4 Spring loaded electromagnetic brake

A spring loaded electromagnetic brake has been used to arrest the rotation of shaft due to back torque of the electric motor in electric only mode. This brake is generally engaged and released when power is supplied through the electromagnetic coil for the hybrid mode. The specifications of the brake are given below and the brake is shown in figure 4.6

Table 4.3: Specifications of electromagnetic brake

Model	Fail Safe Brake Size:165
Voltage	48V
Torque	60Nm
Max Speed	3000rpm
Input Power	50W

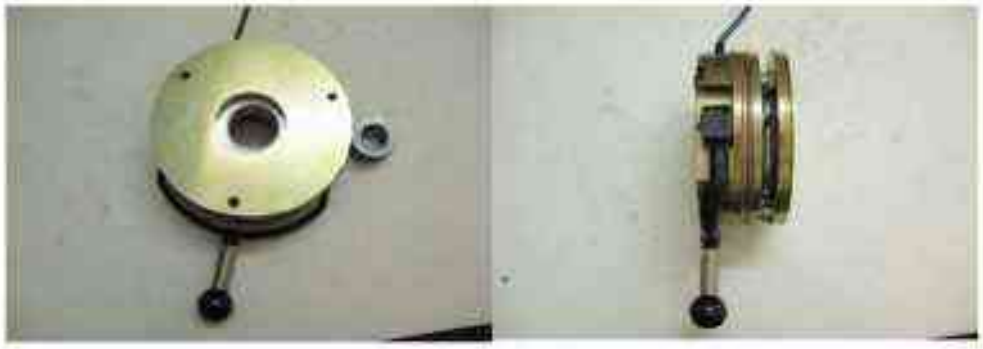

Figure 4.6: Spring loaded electromagnetic brake

4.3.5 Continuous variable transmission (CVT)

The CVT chosen is from a two-wheeled vehicle used in India. The chosen CVT, shown in figure 4.7, can transmit up to 7 hp and is easily available locally. The main components of the CVT are shown in figure 4.7.

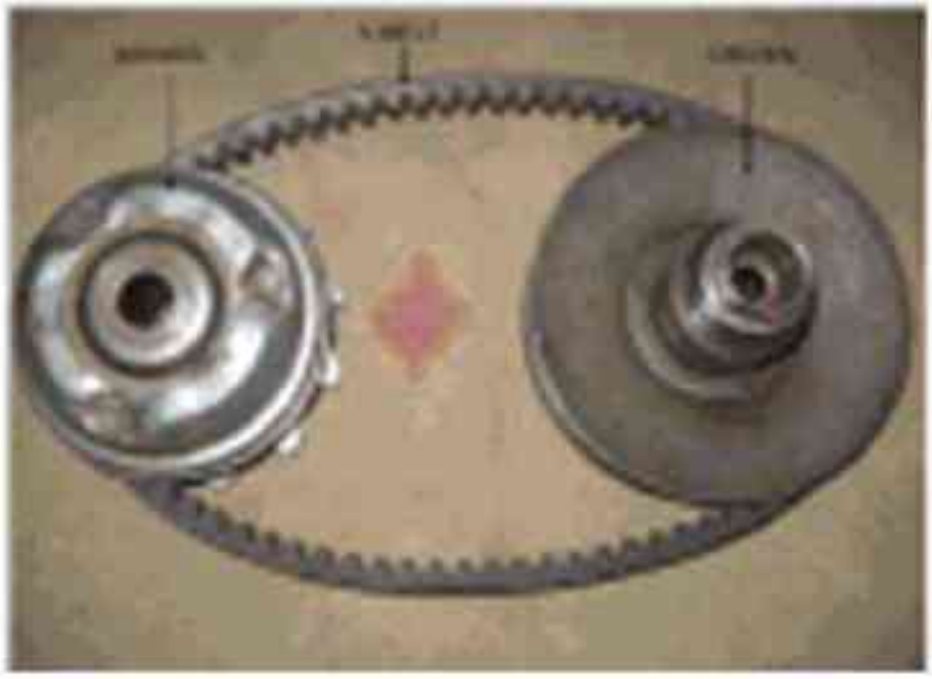

Figure 4.7: CVT showing belt and two pulleys

Figure 4.8: Parts of a CVT from a two-wheeler

4.3.6 Dynamometer

A 10 kW eddy current dynamometer is used for loading the setup and collecting the speed and torque of the engine. The dynamometer is water cooled and various types of loading like ramp, constant etc. The dynamometer used is shown in figure 4.9

Figure 4.9: Eddy current dynamometer

4.4 Experimental procedure

The experiments are done in two modes for both the setups [68] – a) electric only and b) hybrid. For speed addition in the pure electric mode the power to clutch and brake is disabled. The clutch is disengaged and the brake holds the shaft from rotating due to the counter torque. The throttle of electric motor is set to the desired value and then the dynamo meter is loaded by varying the torque linearly and the changes in speed and torque are logged using a data acquisition system on a computer. In the hybrid mode the power to clutch and brake is enabled. The clutch is engaged transmitting the power from IC engine to the stator of the brushless DC hub motor. The brake is disengaged allowing the shaft to rotate freely. The throttle of the IC engine is set to a desired position and the electric motor is set at the same setting as in the only electric mode to compare results.

For torque addition in electric mode the power to clutch and brake is disabled. The clutch is disengaged. The throttle of electric motor is set to the desired value and then the dynamo meter is loaded by varying the torque linearly and the changes in speed and torque are logged on a computer. In the hybrid mode the power to clutch is enabled. The clutch is engaged transmitting the power from IC engine to the gears connected to the rotor of the brushless DC hub motor. The throttle of the IC engine is set to a defined position used in the speed addition test and the electric motor is set at the same position as in the only electric mode to compare results.

4.5 Experimental results and discussion

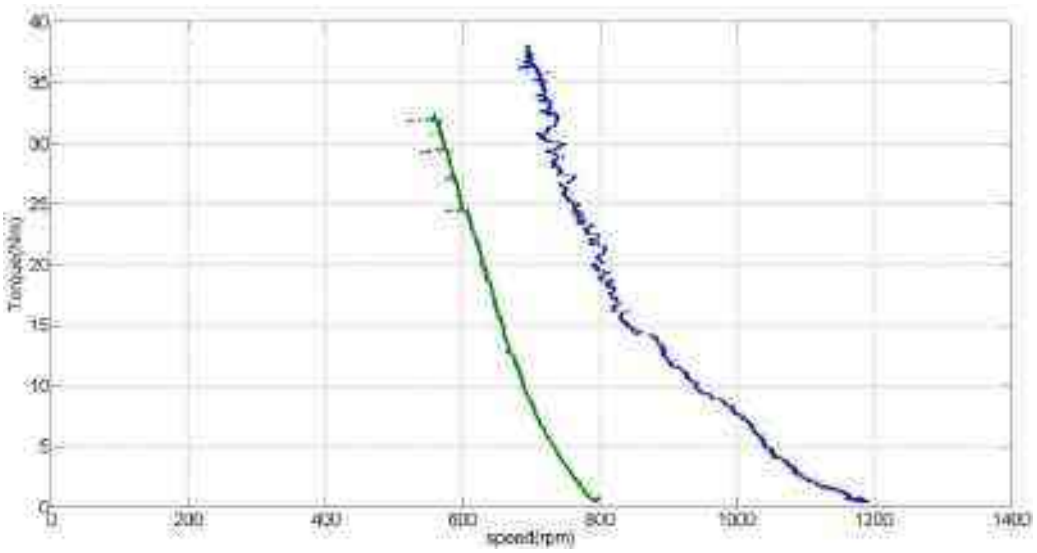

Figure 4.10: Experimental results for speed addition – Case 1

We conducted several experiments – two sample results are shown in this section. As seen in figure 4.10, the initial difference in rpm between DC motor alone and DC motor plus IC engine is about 400. As the load increases, due to the change in the ratio in the CVT, the two curves come closer. After a load of 19 N, the CVT ratio does not change any more and one can see that both the curves are nearly parallel. This clearly demonstrates that addition of power takes place due to the addition of speed.

As seen in figure 4.11, the initial difference in rpm between DC motor alone and DC motor plus IC engine is about 700. As the load increases, due to the change in the ratio in the CVT, the two curves come closer. Due to maximum throttle the CVT does not reach the minimum ratio and hence, the curves are not parallel to each other. Again the experimental results show

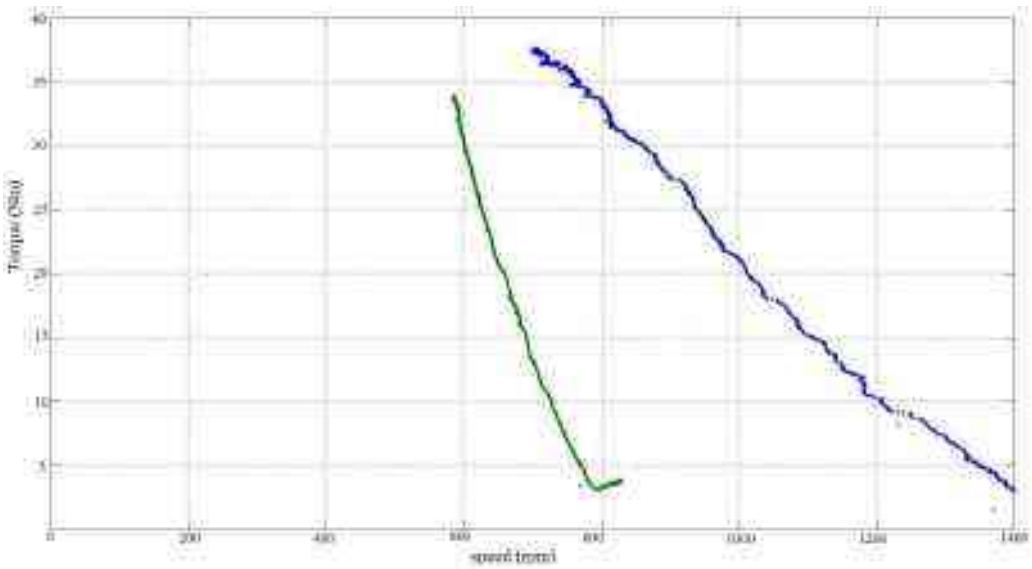

Figure 4.11: Experimental results for speed addition – Case 2

that addition of power takes place due to the addition of speed

4.5.1 Comparative study of speed addition with torque addition

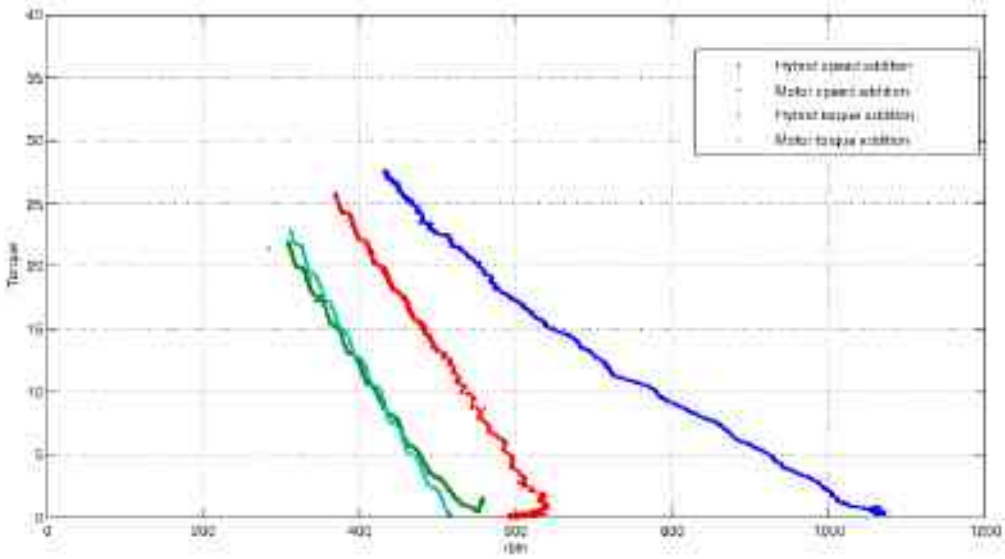

Figure 4.12: Comparison of speed and torque addition

Figure 4.12 shows the experimental results for speed and torque addition at same engine rpm and motor power. It should be noted that the engine used in both the experimental test-beds

is same and the motors used are of same capacity (2 kW). As marked in the figure 4.12, the four curves represent the torque-speed performances in case of speed addition configuration, for torque addition configuration and the torque-speed curve for only the DC motor in both the configurations. As the DC motor is run at the same rpm (500 rpm) for both the configurations, the torque-speed curves for the DC motor almost overlap each other. It can be observed that, for same torques, the speed addition curve gives a higher rpm and this is more pronounced at lower torque levels. This is expected to make the speed addition configuration more efficient.

4.6 Summary

In this Chapter, we have presented the design of the test-bed to explore the novel hybrid architecture where speeds are added at constant torque. The main power components are a 2 kW DC hub motor and a 175 cc single cylinder IC engine. A CVT is connected to the output of the IC engine and the CVT output is connected to the stator of the hub motor through an electromagnetic clutch and brake. This arrangement results in addition of speeds at the wheel output unlike typical parallel hybrid architectures where torque addition takes place. A major advantage of the set up is that there is no need of complicated power transmission – the arrangement of the components is in series even though it is parallel hybrid architecture. The experimental results demonstrate the validity of the speed addition concept.

Chapter 5

Conclusions

5.1 Summary

The study of hybrid powertrain has a very long history going back to 1898 when Porsche built a series hybrid. This thesis proposes a novel hybrid propulsion architecture and the corresponding control strategy for comparing the efficiency of the system with a conventional torque addition hybrid vehicle. The novel architecture has a simple transmission and is shown to give better fuel economy for slow speed, start-stop urban driving prevalent in the crowded cities in emerging economies.

In chapter 2, we presented the actual usage of a commonly used means of transportation in India namely the three-wheeled auto-rickshaw. The GPS based data collected on four different auto-rickshaws over 30 days each is used to calculate statistics of actual usage. It was found that the maximum range of the auto-rickshaw was 137 Km and an average range was 72.6 Km. The average speed was 12.5 Km/h with the driver halting or going very slow (less than 5 Kmph) for more than 60% of the time. This makes the auto-rickshaw an ideal candidate for electric vehicle. Considering the cost and capacity issues of current batteries or energy storage systems, a hybrid system is proposed. The total power required to drive the vehicle and the total torque required required at the wheel along the wheel rpm to drive the vehicle along a drive cycle is obtained from a model developed in this chapter. A novel speed addition hybrid architecture is proposed and described in this chapter.

In chapter 3, two different control strategies are proposed for the speed and conventional torque addition hybrid architectures. The fuel economy under the modified Indian Driving Cycle were obtained using a control strategy based on rule based heuristics and a control strategy

obtained from optimal control derived from dynamic programming. It is shown that the speed addition concept can lead to better fuel economy and the reasons are explained by the location of the operating points on the engine map. In the second part of this chapter, an optimal control strategy is derived using dynamic programming. The state of charge (SOC) in the battery is used a state function, the percentage of hybridization is used as the control function and the fuel consumption is chosen as the cost function. Soft and hard final constraints for SOC to maintain the battery in operating levels are applied. It is shown that the speed addition configuration gives a better fuel economy when compared to that of torque addition configuration. The optimal control strategy using dynamic programming is also applied to the data on the actual movement data of auto-rickshaw in Bangalore city, India. It is observed that the fuel economy of speed addition configuration is better when compared to that of torque addition configuration. It is shown that the fuel economy is primarily dependent on the acceleration and deceleration of the vehicle.

In chapter 4 we describe various components used in the test-bed fabricated to test the concept of speed addition. The detailed specifications of the components used in test-bed, the layout of the components for speed addition and a basic torque addition is shown. Experimental results show an expected shift on the speed axis in hybrid configuration when compared to that of electric motor and the results thus validates the proposed speed addition concept. Comparison of experimental results with those obtained for torque addition show higher power output at lower torque reinforcing the claim that speed addition configuration is suitable for smaller vehicles.

5.2 Scope of future work

The modeling of components used in chapter 2 are the best approximation obtained from the available data of the vehicle. These models can be improved further by considering the mechanical or electronic accessories that can be included into model. Even a emission model can be included to balance the emissions with the fuel consumption by implementing a proper control algorithm. In chapter 3 dynamic programming has been used in obtaining a optimal distribution of load between IC engine and the electric motor for minimizing the fuel consumption. The same can be expanded to include an emission model and obtain a optimal distribution between two power sources to minimize the combination of both fuel consumption and emissions. The concept of dynamic programming cannot be applied in an actual vehicle due to the lack of knowledge of the complete drive cycle in advance. There is a need for a proper supervisory control system with instantaneous optimization that can be developed for speed addition

configuration. In chapter 4 a basic test bed has been created for experimental validation of a concept of speed addition. This can be further extended by implementing the concept of speed addition into an actual vehicle and testing the same to obtain the real world performances.

The speed addition concept can be readily applied for small cars and can be extended for large vehicle by using a different transmission other than a belt CVT. Further work is required to compare the proposed speed addition model with various other available hybrid configurations.

Appendices

Appendix A

Fuel consumption data

The fuel data is for a 185cc single cylinder IC engine. The data shows the brake specific fuel consumption at specific speed and torque output. The speeds are from 1400 to 7974 rpm and the torque are from 0 to 20 Nm. The data was supplied by GM R&D Warren, Michigan, USA. The fuel data has been rounded off to the integer value to properly fit into a page.

Appendix B

Autonomie Result

AUTONOMIE

Argonne

Summary

Vehicle

Vehicle Propulsion Architecture

System Name		parallel_posthyb_hev_autoshare_2out_reduce
Simulation Folder		2010_0706_0120_19_000
Process Name		EEF Cycle
Cycle Name		EEF
Distance Traveled	km	1.0123
Cycle Distance	km	1.0167
Start Time	s	0
End Time	s	192
Percent Time Trace Missed by 2mph	%	0
Driver Performance Index (SAE J2951)		-0.16034
Percentage of energy spent during idling	%	0.020002
Fuel Economy	km/l	38.5956
Fuel Consumption	l/100km	2.5909
CO2 Emission	g/mile	99.5763
Load Specific Fuel Economy	l/m/kg	2.5802e-07
Load Specific Fuel Consumption	l/100km/ton	25.9001
Load Specific CO2 Emission	g/km/ton	618.7599
Fuel Economy Gasoline Equivalent	km/l	38.2296
Electrical Consumption	w.h/mile	8.0002
Initial SOC	%	70
Final SOC	%	57.0176
Delta SOC	%	-12.9823
Percent Regen Braking at Battery	%	99.8161
Percent Regen Braking at Wheel	%	99.6996
Percent of energy used for the cycle from regen	%	2.8356
Regen Braking Energy Recovered at Battery	w.h	2.0773
Regen Braking Energy Available at Wheel	w.h	3.37
Total Braking Energy at Wheel	w.h	3.7153

Vehicle Propulsion Architecture

Engine

Bidirectional Efficiency	%	34.8654
Unidirectional Energy In	W.h	234.6443
Unidirectional Energy Out	W.h	81.5822

Mechanical Accessory

Bidirectional Efficiency	%	100
Unidirectional Energy In	W.h	81.5822
Unidirectional Energy Out	W.h	81.5822

Clutch/Torque Converter

Bidirectional Efficiency	%	99.7833
Unidirectional Energy In	W.h	81.5822
Unidirectional Energy Out	W.h	81.3744

Gearbox

Bidirectional Efficiency	%	90.4668
Unidirectional Energy In	W.h	81.3744
Unidirectional Energy Out	W.h	73.6068

Final Drive

Bidirectional Efficiency	%	97.8056
Unidirectional Energy In	W.h	72.9683
Unidirectional Energy Out	W.h	70.9815

Wheel

Bidirectional Efficiency	%	98.3596
Unidirectional Energy In	W.h	70.9815
Unidirectional Energy Out	W.h	81.4338

Chassis

Bidirectional Efficiency	%	28.3594
Unidirectional Energy In	W.h	51.4338
Unidirectional Energy Out	W.h	0.86385

Energy Storage

Bidirectional Efficiency	%	87.2365
Unidirectional Energy In	W.h	5.057
Unidirectional Energy Out	W.h	4.1373

Motor

Bidirectional Efficiency	%	81.9469
Unidirectional Energy In	W.h	1.3089
Unidirectional Energy Out	W.h	-0.83248

Power Converter

Bidirectional Efficiency	%	95
Unidirectional Energy In	W.h	2.8089
Unidirectional Energy Out	W.h	2.7083

Electrical Accessory

Bidirectional Efficiency	%	0
Unidirectional Energy In	W.h	2.7083
Unidirectional Energy Out	W.h	0

Energy

Vehicle Propulsion Architecture

Engine

Unidirectional Energy In	W.h	234.0443
Unidirectional Energy Out	W.h	81.5522

Mechanical Accessory

Unidirectional Energy In	W.h	81.5522
Unidirectional Energy Out	W.h	81.5522

Clutch/Torque Converter

Unidirectional Energy In	W.h	81.5522
Unidirectional Energy Out	W.h	81.3744

Gearbox

Unidirectional Energy In	W.h	81.3744
Unidirectional Energy Out	W.h	73.8698

Final Drive

Unidirectional Energy In	W.h	72.9583
Unidirectional Energy Out	W.h	70.5815

Wheel

Unidirectional Energy In	W.h	70.5815
Unidirectional Energy Out	W.h	61.4338

Chassis

Unidirectional Energy In	W.h	61.4338
Unidirectional Energy Out	W.h	0.86385

Energy Storage

Unidirectional Energy In	W.h	3.557
Unidirectional Energy Out	W.h	4.1375

Motor

Unidirectional Energy In	W.h	1.3091
Unidirectional Energy Out	W.h	-0.63246

Power Converter

Unidirectional Energy In	W.h	2.5509
Unidirectional Energy Out	W.h	2.7003

Electrical Accessory

Unidirectional Energy In	W.h	2.7003
Unidirectional Energy Out	W.h	0

Warnings

Simulation Checks

Vehicle Warnings

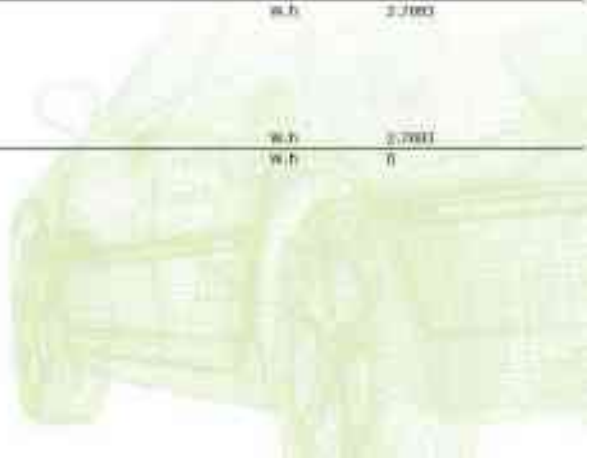

References

[1] D. D. Doniger, *Dangerous Addiction: Ending America's Oil Dependence*. Natural Resources Defense Council, 2003. 1

[2] M. Abolhassani, P. Acharya, P. Asadi, T. Ashmun, S. Campbell, D. Dorsey, D. Hoelscher, P. Niazi, L. Palma, L. Parsa, *et al.*, "Impact of hybrid electric vehicles on the world's petroleum consumption and supply," tech. rep., SAE Technical Paper, 2003. 1

[3] R. A. Weinstock, P. T. Krein, and R. A. White, "Optimal sizing and selection of hybrid electric vehicle components," in *Power Electronics Specialists Conference, 1993. PESC'93 Record., 24th Annual IEEE*, pp. 251–256, IEEE, 1993. 1

[4] B. C. Chan, "The state of the art of electric, hybrid, and fuel cell vehicles," *Proceedings of the IEEE*, vol. 95, no. 4, pp. 704–718, 2007. 2, 3

[5] K. G. Høyer, "The history of alternative fuels in transportation: The case of electric and hybrid cars," *Utilities Policy*, vol. 16, no. 2, pp. 63–71, 2008. 2

[6] D. A. Kirsch, *The electric vehicle and the burden of history*. Rutgers University Press, 2000. 2

[7] L. Situ, "Electric vehicle development: the past, present & future," in *Power Electronics Systems and Applications, 2009. PESA 2009. 3rd International Conference on*, pp. 1–3, IEEE, 2009. 2

[8] E. H. Wakefield, *History of the Electric Automobile-Hybrid Electric Vehicles*, vol. 187. Society of Automotive Engineers, 1998. 3

[9] M. P. O'Keefe and T. Markel, "Dynamic programming applied to investigate energy management strategies for a plug-in hev," tech. rep., National Renewable Energy Laboratory, 2006. 8

[10] A. Brahma, Y. Guezennec, and G. Rizzoni, "Optimal energy management in series hybrid electric vehicles," in *American Control Conference, 2000. Proceedings of the 2000*, vol. 1, pp. 60–64, IEEE, 2000. 8

[11] L. Johannesson, M. Åsbogård, and B. Egardt, "Assessing the potential of predictive control for hybrid vehicle powertrains using stochastic dynamic programming," *Intelligent transportation systems, IEEE transactions on*, vol. 8, no. 1, pp. 71–83, 2007. 8

[12] L. V. Pérez, G. R. Bossio, D. Moitre, and G. O. García, "Optimization of power management in an hybrid electric vehicle using dynamic programming," *Mathematics and Computers in Simulation*, vol. 73, no. 1, pp. 244–254, 2006. 8

[13] R. Bellman, "On the theory of dynamic programming," *Proceedings of the National Academy of Sciences*, vol. 38, no. 8, pp. 716–719, 1952. 8

[14] H. J. Sussmann and J. C. Willems, "300 years of optimal control: from the brachystochrone to the maximum principle," *Control Systems, IEEE*, vol. 17, no. 3, pp. 32–44, 1997. 9

[15] L. Pontryagin, V. Boltyanskii, R. Gamkrelidze, and E. Mishchenko, "Matematicheskaya teoriya optimalnykh prozessov. fizmatgiz, moscow. translated into english. the mathematical theory of optimal processes," 1962. 9

[16] D. P. Bertsekas, D. P. Bertsekas, D. P. Bertsekas, and D. P. Bertsekas, *Dynamic programming and optimal control*, vol. 1. Athena Scientific Belmont, MA, 1995. 9, 46, 48

[17] H. P. Geering, *Optimal control with engineering applications*, vol. 113. Springer, 2007. 9

[18] M. Anatone, R. Cipollone, A. Donati, and A. Sciarretta, "Control-oriented modeling and fuel optimal control of a series hybrid bus," tech. rep., SAE Technical Paper, 2005. 9

[19] X. Wei, L. Guzzella, V. Utkin, and G. Rizzoni, "Model-based fuel optimal control of hybrid electric vehicle using variable structure control systems," *Journal of dynamic systems, measurement, and control*, vol. 129, no. 1, pp. 13–19, 2007. 9

[20] R. Cipollone and A. Sciarretta, "Analysis of the potential performance of a combined hybrid vehicle with optimal supervisory control," in *Computer Aided Control System Design, 2006 IEEE International Conference on Control Applications, 2006 IEEE International Symposium on Intelligent Control, 2006 IEEE*, pp. 2802–2807, IEEE, 2006. 9

[21] G. Paganelli, T. Guerra, S. Delprat, J. Santin, M. Delhom, and E. Combes, "Simulation and assessment of power control strategies for a parallel hybrid car," *Proceedings of the Institution of Mechanical Engineers, Part D: Journal of Automobile Engineering*, vol. 214, no. 7, pp. 705–717, 2000. 10

[22] B. Gu and G. Rizzoni, "An adaptive algorithm for hybrid electric vehicle energy management based on driving pattern recognition," in *ASME 2006 International Mechanical Engineering Congress and Exposition*, pp. 249–258, American Society of Mechanical Engineers, 2006. 10

[23] E. Cacciatori, N. D. Vaughan, and J. Marco, "Energy management strategies for a parallel hybrid electric powertrain: Fuel economy optimisation with driveability requirements," in *Hybrid Vehicle Conference, IET The Institution of Engineering and Technology, 2006*, pp. 157–172, IET, 2006. 11

[24] X. He, M. Parten, and T. Maxwell, "Energy management strategies for a hybrid electric vehicle," in *Vehicle Power and Propulsion, 2005 IEEE Conference*, pp. 536–540, IEEE, 2005. 11

[25] T. Hofman, M. Steinbuch, R. Van Druten, and A. Serrarens, "Rule-based energy management strategies for hybrid vehicles," *International Journal of Electric and Hybrid Vehicles*, vol. 1, pp. 71–94, 2007. 11

[26] C.-C. Lin, H. Peng, J. W. Grizzle, and J.-M. Kang, "Power management strategy for a parallel hybrid electric truck," *Control Systems Technology, IEEE Transactions on*, vol. 11, pp. 839–849, 2003. 11

[27] B. Wu, C.-C. Lin, Z. Filipi, H. Peng, and D. Assanis, "Optimal power management for a hydraulic hybrid delivery truck," *Vehicle System Dynamics*, vol. 42, no. 1-2, pp. 23–40, 2004. 11

[28] N. Kim, S. Cha, and H. Peng, "Optimal control of hybrid electric vehicles based on pontryagin's minimum principle," *Control Systems Technology, IEEE Transactions on*, vol. 19, no. 5, pp. 1279–1287, 2011. 11

[29] O. Bitsche and G. Gutmann, "Systems for hybrid cars," *Journal of Power Sources*, vol. 127, no. 1, pp. 8–15, 2004. 11

[30] H. L. MacLean and L. B. Lave, "Evaluating automobile fuel/propulsion system technologies," *Progress in energy and combustion science*, vol. 29, no. 1, pp. 1–69, 2003. 11

[31] E. Tate, M. O. Harpster, and P. J. Savagian, *The electrification of the automobile: from conventional hybrid, to plug-in hybrids, to extended-range electric vehicles*. Citeseer, 2008. 11

[32] A. Sharma and A. Roychowdhury, "Slow murder: the deadly story of vehicular pollution in india.," *Center for Science and Environment (CSE), New Delhi*, 1996. 11

[33] S. M. Lukic, P. Mulhall, G. Choi, M. Naviwala, S. Nimmagadda, and A. Emadi, "Usage pattern development for three-wheel auto rickshaw taxis in india," in *Vehicle Power and Propulsion Conference, 2007. VPPC 2007. IEEE*, pp. 610–616, IEEE, 2007. 11, 64

[34] "Dg-100 gps + data logger." (Date last accessed 28-July-2016). 15

[35] D. W. Gao, C. Mi, and A. Emadi, "Modeling and simulation of electric and hybrid vehicles," *Proceedings of the IEEE*, vol. 95, no. 4, pp. 729–745, 2007. 19

[36] G. Rizzoni, L. Guzzella, and B. M. Baumann, "Unified modeling of hybrid electric vehicle drivetrains," *Mechatronics, IEEE/ASME Transactions on*, vol. 4, no. 3, pp. 246–257, 1999. 19

[37] K. L. Butler, M. Ehsani, and P. Kamath, "A matlab-based modeling and simulation package for electric and hybrid electric vehicle design," *Vehicular Technology, IEEE Transactions on*, vol. 48, no. 6, pp. 1770–1778, 1999. 19

[38] N. R. C. U. T. R. B. C. for the National Tire Efficiency Study, *Tires and Passenger Vehicle Fuel Economy: Informing Consumers, Improving Performance*, vol. 286. Transportation Research Board, 2006. 20

[39] L. Guzzella and A. Sciarretta, *Vehicle propulsion systems*, vol. 1. Springer, 2007. 20, 27

[40] W.-h. Hucho and G. Sovran, "Aerodynamics of road vehicles," *Annual review of fluid mechanics*, vol. 25, no. 1, pp. 485–537, 1993. 22

[41] E. Hendricks, "Engine modelling for control applications: a critical survey," *Meccanica*, vol. 32, no. 5, pp. 387–396, 1997. 22

[42] D. R. Buttsworth, *Spark ignition internal combustion engine modelling using Matlab*. Faculty of Engineering & Surveying, University of Southern Queensland, 2002. 22

[43] Y. Ra and R. D. Reitz, "A reduced chemical kinetic model for ic engine combustion simulations with primary reference fuels," *Combustion and Flame*, vol. 155, no. 4, pp. 713–738, 2008. 22

[44] G. Carbone, L. Mangialardi, B. Bonsen, C. Tursi, and P. Veenhuizen, "Cvt dynamics: Theory and experiments," *Mechanism and Machine Theory*, vol. 42, no. 4, pp. 409–428, 2007. 24

[45] N. Srivastava and I. Haque, "A review on belt and chain continuously variable transmissions (cvt): Dynamics and control," *Mechanism and machine theory*, vol. 44, no. 1, pp. 19–41, 2009. 24

[46] L. Guzzella and A. Amstutz, "The qss toolbox manual," *ETH Zürich, http://www. imrt. ethz. ch/research/qss*, 2005. 24

[47] J. F. Manwell and J. G. McGowan, "Lead acid battery storage model for hybrid energy systems," *Solar Energy*, vol. 50, no. 5, pp. 399–405, 1993. 25

[48] Z. Chehab, L. Serrao, Y. G. Guezennec, and G. Rizzoni, "Aging characterization of nickel: Metal hydride batteries using electrochemical impedance spectroscopy," in *ASME 2006 International Mechanical Engineering Congress and Exposition*, pp. 343–349, American Society of Mechanical Engineers, 2006. 26

[49] M. Dubarry, V. Svoboda, R. Hwu, and B. Y. Liaw, "Capacity and power fading mechanism identification from a commercial cell evaluation," *Journal of Power Sources*, vol. 165, no. 2, pp. 566–572, 2007. 26

[50] ARAI, "Document on test method, testing equipment and related procedures for testing type approval and conformity of production of vehicles for emission as per cmv rules 115, 116 and 126." 27

[51] E. Tzirakis, K. Pitsas, F. Zannikos, and S. Stournas, "Vehicle emissions and driving cycles: comparison of the athens driving cycle (adc) with ece-15 and european driving cycle (edc)," *Global NEST Journal*, vol. 8, no. 3, pp. 282–290, 2006. 27

[52] P. Pisu, C.-G. Cantemir, N. Dembski, G. Rizzoni, L. Serrao, J. R. Josephson, and J. Russell, "Evaluation of powertrain solutions for future tactical truck vehicle systems," in *Defense and Security Symposium*, pp. 62280D–62280D, International Society for Optics and Photonics, 2006. 28

[53] X. Wei, P. Pisu, G. Rizzoni, and S. Yurkovich, "Dynamic modeling of a hybrid electric drivetrain for fuel economy, performance and driveability evaluations," in *ASME 2003 international mechanical engineering congress and exposition*, pp. 443–450, American Society of Mechanical Engineers, 2003. 28

[54] M. Ehsani, Y. Gao, and A. Emadi, *Modern electric, hybrid electric, and fuel cell vehicles: fundamentals, theory, and design*. CRC press, 2009. 30

[55] A. Ghosal, *Robotics: fundamental concepts and analysis*. Oxford University Press, 2006. 33

[56] A. N. Laboratories, "Autonomie." (Date last accessed 28-July-2016). 34

[57] T. M. Corp., "A guide to hybrid synergy drive." (Date last accessed 28-July-2016). 35

[58] J. Moreno, M. E. Ortúzar, and J. W. Dixon, "Energy-management system for a hybrid electric vehicle, using ultracapacitors and neural networks," *IEEE transactions on Industrial Electronics*, vol. 53, no. 2, pp. 614–623, 2006. 36

[59] R. V. Gopal and A. P. Rousseau, "System analysis using multiple expert tools," tech. rep., SAE Technical Paper, 2011. 44

[60] A. Sciarretta and L. Guzzella, "Control of hybrid electric vehicles," *Control systems, IEEE*, vol. 27, no. 2, pp. 60–70, 2007. 47

[61] R. E. Bellman and S. E. Dreyfus, *Applied dynamic programming*. Princeton university press, 2015. 48

[62] A. Bemporad, P. Borodani, and M. Mannelli, "Hybrid control of an automotive robotized gearbox for reduction of consumptions and emissions," in *Hybrid Systems: Computation and Control*, pp. 81–96, Springer, 2003. 48

[63] F. L. Lewis and V. L. Syrmos, *Optimal control*. John Wiley & Sons, 1995. 48

[64] R. Luus, *Iterative dynamic programming*. CRC Press, 2000. 48

[65] O. Sundström, D. Ambühl, and L. Guzzella, "On implementation of dynamic programming for optimal control problems with final state constraints," *Oil & Gas Science and Technology–Revue de lInstitut Français du Pétrole*, vol. 65, no. 1, pp. 91–102, 2010. 49, 50

[66] "Kelly controllers hubmotor 48v 2kw." (Date last accessed 28-July-2016). 62

[67] "Electromagnetic shaft mounted clutch and spring-applied failsafe brake-type." (Date last accessed 28-July-2016). 65

[68] M. Raghavan, R. Chanumolu, and F. Park, "Novel propulsion and energy recharge architectures for urban vehicles," in *proc. of EVS*, 2015. 68